

Generation of a CRF₁-Cre transgenic rat and the role of central amygdala CRF₁ cells in nociception and anxiety-like behavior

Marcus M Weera^{1*}, Abigail E Agoglia², Eliza Douglass², Zhiying Jiang³, Shivakumar Rajamanickam³, Rosetta S Shackett¹, Melissa A Herman^{2,4†}, Nicholas J Justice^{3,5†}, Nicholas W Gilpin^{1,6,7,8†}

¹Department of Physiology, Louisiana State University Health Sciences Center, New Orleans, United States; ²Department of Pharmacology, University of North Carolina, Chapel Hill, United States; ³Institute of Molecular Medicine, University of Texas Health Sciences Center, Houston, United States; ⁴Bowles Center for Alcohol Studies, University of North Carolina, Chapel Hill, United States; ⁵Department of Integrative Biology and Pharmacology, McGovern Medical School at UT Health, Houston, United States; ⁶Neuroscience Center of Excellence, Louisiana State University Health Sciences Center, New Orleans, United States; ⁷Alcohol & Drug Abuse Center of Excellence, Louisiana State University Health Sciences Center, New Orleans, United States; ⁸Southeast Louisiana VA Healthcare System (SLVHCS), New Orleans, United States

*For correspondence:
mweera@lsuhsc.edu

†These authors contributed equally to this work

Competing interest: The authors declare that no competing interests exist.

Funding: See page 23

Preprinted: 23 February 2021

Received: 24 February 2021

Accepted: 06 April 2022

Published: 07 April 2022

Reviewing Editor: Matthew N Hill, University of Calgary, Canada

© Copyright Weera et al. This is an open-access article, free of all copyright, and may be freely reproduced, distributed, transmitted, modified, built upon, or otherwise used by anyone for any lawful purpose. The work is made available under the [Creative Commons CC0 public domain dedication](https://creativecommons.org/licenses/by/4.0/).

Abstract Corticotropin-releasing factor type-1 (CRF₁) receptors are critical to stress responses because they allow neurons to respond to CRF released in response to stress. Our understanding of the role of CRF₁-expressing neurons in CRF-mediated behaviors has been largely limited to mouse experiments due to the lack of genetic tools available to selectively visualize and manipulate CRF₁⁺ cells in rats. Here, we describe the generation and validation of a transgenic CRF₁-Cre^{-tdTomato} rat. We report that *Crrh1* and *Cre* mRNA expression are highly colocalized in both the central amygdala (CeA), composed of mostly GABAergic neurons, and in the basolateral amygdala (BLA), composed of mostly glutamatergic neurons. In the CeA, membrane properties, inhibitory synaptic transmission, and responses to CRF bath application in ^{tdTomato} neurons are similar to those previously reported in GFP⁺ cells in CRFR1-GFP mice. We show that stimulatory DREADD receptors can be targeted to CeA CRF₁⁺ cells via virally delivered Cre-dependent transgenes, that transfected Cre^{-tdTomato} cells are activated by clozapine-n-oxide in vitro and in vivo, and that activation of these cells in vivo increases anxiety-like and nociceptive behaviors. Outside the amygdala, we show that Cre^{-tdTomato} is expressed in several brain areas across the brain, and that the expression pattern of Cre^{-tdTomato} cells is similar to the known expression pattern of CRF₁ cells. Given the accuracy of expression in the CRF₁-Cre rat, modern genetic techniques used to investigate the anatomy, physiology, and behavioral function of CRF₁⁺ neurons can now be performed in assays that require the use of rats as the model organism.

Editor's evaluation

This manuscript details the generation and characterization of a new transgenic rat line presenting an exciting new tool to the field.

Introduction

Corticotropin-releasing factor (CRF) is a 41 amino acid neuropeptide that acts on various cell populations in the brain and elicits stress-related behavioral (e.g. anxiety) and physiological (e.g. sympathomimetic) responses (Vale et al., 1981; Henckens et al., 2016). In the hypothalamic-pituitary-adrenal (HPA) axis, CRF released by neurons in the paraventricular nucleus of the hypothalamus (PVN) into the hypophyseal portal system stimulates adrenocorticotrophic hormone (ACTH) release from the pituitary, which in turn stimulates release of glucocorticoids from the adrenal cortex. Glucocorticoids released into the circulatory system serve as effectors of the HPA axis by modulating various physiological (e.g. cardiovascular, respiratory, and immune) functions (Smith and Vale, 2006). Extrahypothalamic CRF neurons are located in many brain areas that modulate affective states and behaviors, such as the amygdala, cortex, hippocampus, midbrain, and locus coeruleus (Peng et al., 2017). Among these brain areas, the extended amygdala, particularly the central amygdala (CeA) and bed nucleus of stria terminalis (BNST), contain the highest densities of CRF neurons (Peng et al., 2017).

CRF type-1 (CRF₁) receptors are G_s- or G_q-coupled metabotropic receptors (Milan-Lobo et al., 2009; Wanat et al., 2008) that are highly expressed in brain areas that contain high densities of CRF fibers and/or CRF neurons, including the CeA, BNST, and medial amygdala. CRF signaling via CRF₁ modulates neurophysiological processes underlying stress reactivity, anxiety-related behaviors, learning and memory processes including fear acquisition and/or expression, pain signaling, and addiction-related behaviors (see reviews by Dedic et al., 2018; Henckens et al., 2016). Therefore, elucidation of the circuit-specific and cell-specific mechanisms by which CRF₁ signaling mediates these processes represents an important avenue of research for understanding behaviors related to stress, anxiety, fear, pain, and addiction.

The central amygdala (CeA) is a key nucleus in modulating affective states and behaviors related to stress, anxiety, fear, pain, and addiction (Gilpin et al., 2015). Functionally, the CeA serves as a major output nucleus of the amygdala and can be anatomically divided into lateral (CeAl) and medial (CeAm) subdivisions (Duvarci and Pare, 2014). In mice and rats, CRF-expressing (CRF⁺) neurons are densely localized to the CeAl, whereas CRF₁-expressing (CRF₁⁺) neurons are mostly localized to the CeAm (Day et al., 1999; Jolkkonen and Pitkänen, 1998; Justice et al., 2008; Pomrenze et al., 2015). In addition to receiving CRF input from CRF⁺ neurons in the CeAl, the CeAm receives CRF inputs from distal brain areas such as the bed nucleus of stria terminalis (BNST) (Dabrowska et al., 2016) and dorsal raphe nucleus (Commons et al., 2003). CeA CRF₁ signaling plays an important role in modulating affective states and behaviors. For example, pharmacological blockade of CeA CRF₁ attenuates stress-induced increases in anxiety-like behavior (Henry et al., 2006), nociception (Itoga et al., 2016), and alcohol drinking (Roberto et al., 2010; Weera et al., 2020), as well as fear acquisition and expression (Sanford et al., 2017). Work using transgenic CRF and CRF₁ reporter and Cre-driver mice have shed light on circuit- and cell-specific mechanisms by which CeA CRF⁺ and CRF₁⁺ cells mediate affective behaviors (e.g. Fadok et al., 2017; Sanford et al., 2017). However, mice have a limited behavioral repertoire when compared to rats, making the study of more complex behaviors (e.g. drug self-administration and social interaction; Homberg et al., 2017) difficult.

Here, we describe the generation of a novel CRF₁-Cre^{-td}Tomato transgenic rat line. We show that *Crrh1* and *iCre* mRNA are expressed in the same neurons in the CeA and BLA using hybridization histochemistry. In the CeA, we show that ^{td}Tomato⁺ neurons are abundant in the CeAm, and that they are surrounded and in contact with CRF-containing puncta. We recorded membrane properties, inhibitory synaptic transmission, and spontaneous firing in CeA CRF₁-Cre^{-td}Tomato cells and show that these cells are sensitive to CRF. In addition, we show that Cre-dependent DREADD receptors can be targeted for expression by CeA CRF₁ cells such that DREADD stimulation of CRF₁⁺ CeA neurons increases nociception and anxiety-like behaviors, recapitulating prior work using pharmacological strategies. Outside the amygdala, we analyzed the expression of CRF₁-Cre^{-td}Tomato cells in several brain areas across the rostrocaudal axis and show that these cells are found in brain areas known to contain CRF₁-expressing cells. These anatomical, electrophysiological, and functional data support the utility of this CRF₁-Cre^{-td}Tomato transgenic rat line for the study of CRF₁ neural circuit function, and will be an important new resource that will complement CRFR1:GFP and CRFR1:Cre mice (Justice et al., 2008; Jiang et al., 2018; Sanford et al., 2017), and CRF-Cre rats (Pomrenze et al., 2015) for the study of CRF signaling in physiology and behavior.

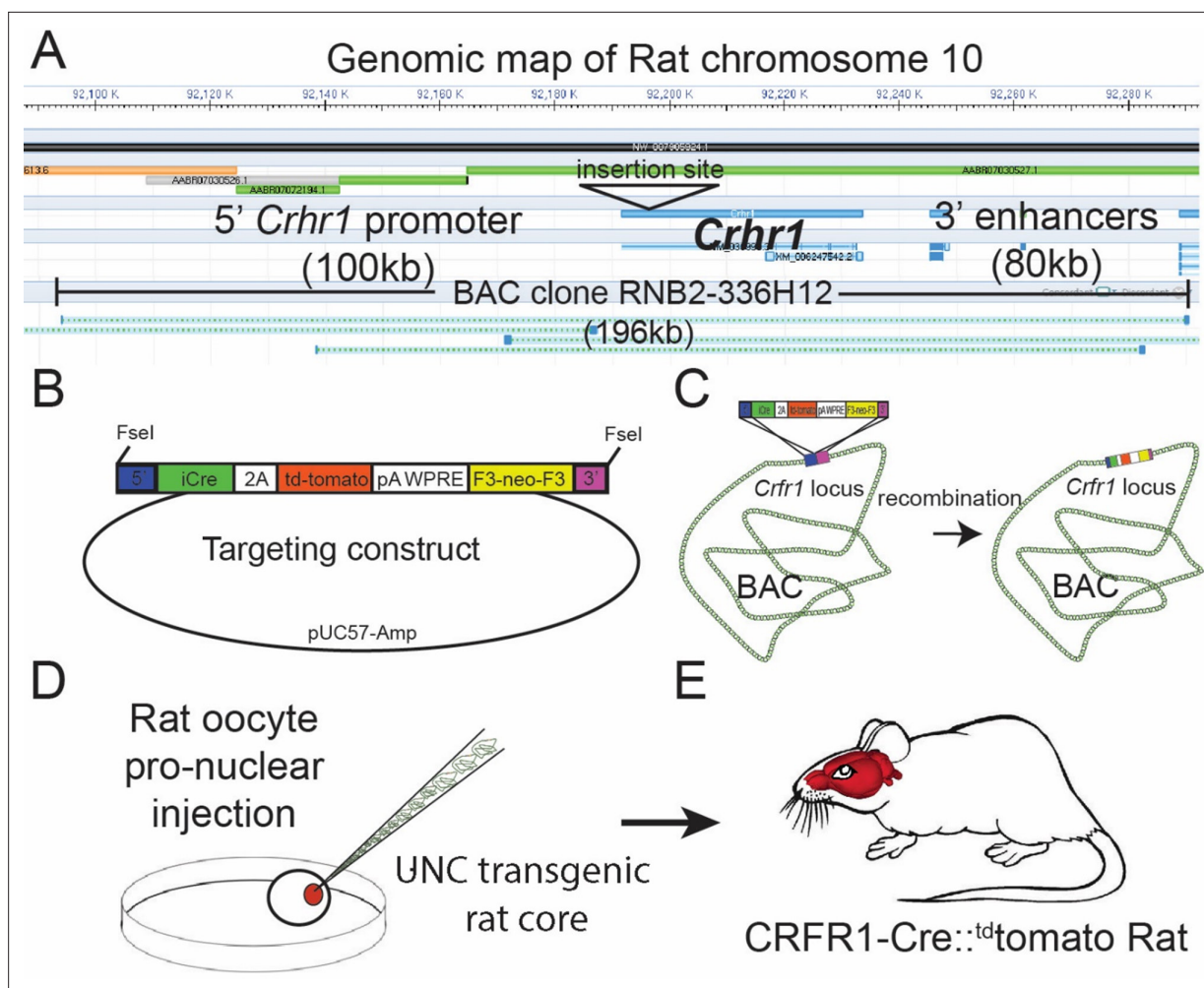


Figure 1. Design of the *Crhr1*-Cre2aTom BAC transgene. (A) *Crhr1* is located on chromosome 10 in the rat. A BAC clone containing 196 kb of DNA surrounding the *Crhr1* coding region includes 100 kb of upstream and 80 kb of downstream DNA, where the majority of promoter and enhancer sequences that control *Crhr1* expression are located, was obtained (Riken, RNB2-336H12). There are no other sequences within this 196 kb DNA clone have been annotated as coding sequences for genes other than *Crhr1*. (B) A transgene containing 5' (blue) and 3' (magenta) targeting sequences, a bicistronic iCre 2A fused tdTomato (red) sequence, 3' polyA/WPRE stabilizing sequence, and a F3 flanked neomycin resistance sequence (yellow) was constructed then transformed into *E. coli* containing the RNB2-336H12 BAC construct. (C) Using recombineering techniques we isolated BAC clones in which targeted insertion of the transgene at the translation start site of *Crhr1* (ATG) was confirmed by PCR/sequencing. A single Bacterial clone containing the transgene inserted BAC was sent to the UNC transgenic facility where BAC DNA was purified and injected into single cell, fertilized rat oocytes. Two independent rat lines were recovered in which the entire BAC sequence (confirmed by PCR) was inserted into genomic DNA, of which one line displayed transgenic expression in a pattern representative of known *Crhr1* expression patterns.

Results

Generation of CRF₁-Cre^{tdTomato} rats and validation of iCre (T^dTomato) expression in CRF₁-expressing cells in the CeA

Design of CRF₁-Cre bacterial artificial chromosome (BAC) transgene

Please refer to **Figure 1** for a schematic of the BAC generation. The design of the CRF₁:Cre rat BAC transgene is similar to the design used to generate CRFR1:Cre BAC transgenic mice (**Jiang et al., 2018**), with the exception that a BAC clone from rat was used (clone RNB2-336H12 from Riken Rat genomic BAC library). The BAC clone used lacks any other identified protein encoding genetic sequences, reducing the possibility that other genes will be expressed from BAC when introduced into the rat genome. We obtained the RNB2-336H12 clone from the Riken Rat BAC clone collection (**STAR Consortium et al., 2008**). This BAC was inserted using recombineering techniques such that

sequences encoding *Crhr1* were replaced, beginning at the translation ATG start site, with sequences encoding a bicistronic *iCre-2A-^{td}Tomato* transgene (**Figure 1C**). *iCre* is a codon-optimized Cre that produces consistent Cre activity (Koresawa et al., 2000). ^{td}Tomato encodes a red fluorescent protein that allows cells expressing the transgene to be visualized (Shaner et al., 2004). The poly A and WPRE sequences stabilize the mRNA to achieve more robust expression (Glover et al., 2002). To insert the *iCre-p2A-tdTomato* cassette into the BAC, we transformed bacterial cells that contain the BAC with a helper plasmid (Portmage-4) which contains a heatshock-inducible element that drives expression of lambda red recombinase and confers chloramphenicol resistance (Liu et al., 2003). These cells were then transformed with the *iCre-p2A-tdTomato* homology arm targeting cassette, after a 15 min heatshock. Cells were selected on kanamycin (for neoR) and colonies were screened by PCR for insertion of the cassette at the site of *Crhr1* in the BAC. BAC DNA from a single clone that contained the correct insertion was purified, then transformed into EL250 cells, which carry an arabinose inducible flipase construct. Cultures of EL250 carrying the inserted BAC were induced to express flp recombinase by incubating in L-arabinose for 1 hr, then selected on ampicillin (the resistance of the BAC) and screened for loss of kanamycin resistance (removed by flp recombinase; **Figure 1**). Colonies were PCR screened to confirm that they contained BAC DNA containing the *Cre-2A-Tom* transgene inserted in the *Crhr1* locus, and lacked the f3 flanked neoR cassette. A single bacterial clone containing the final full-length inserted BAC construct was sent to the University of North Carolina (UNC) Transgenic Core, where BAC DNA was purified, checked for integrity by DNA laddering with EcoR1 and XbaI followed by pulsed-gel electrophoresis, and by PCR, linearized, then injected into single-cell Wistar rat oocytes.

Generation of transgenic rats

Transgenic rats were generated by the UNC Transgenic Core by injecting single-cell rat oocytes with the modified BAC described above (**Figure 1D and E**). DNA from F1 offspring were tested for the presence of the introduced BAC transgene using PCR. Complete BAC insertion was determined using four primer sets representing unique junctions in the BAC. Two animals containing BAC insertions were further tested using this procedure and were found to contain the entire BAC sequence. Transgenic rats were first outcrossed to wildtype Wistar animals, then intercrossed to maximize the genetic similarity of transgenic offspring. Transgenic animals were generated on a Wistar background because Wistar rats are commonly used in models of alcohol and substance use disorders, and other models of behavioral and physiological disorders.

Validation of *iCre* (^{td}Tomato) expression in CeA CRF₁ cells

The purpose of this experiment was to determine the pattern of ^{td}Tomato protein expression and *Crhr1* and *iCre* mRNA expression within the CeA. Immunohistochemical labeling of ^{td}Tomato in the amygdala showed that ^{td}Tomato⁺ cells were located in the lateral, basolateral, central, and medial amygdala (**Figure 2A**). Within the CeA, ^{td}Tomato⁺ cells were found to be concentrated in the CeAm, whereas the CeAl was largely devoid of ^{td}Tomato⁺ cells (**Figure 2B**).

We used RNAscope ISH to test the hypothesis that *Crhr1* and *iCre* mRNA are highly colocalized within the CeA. ^{td}Tomato mRNA was not probed because *iCre* and ^{td}Tomato are expressed as a single polypeptide (*iCre-2A-tdTomato*) that is cleaved at the 2 A site. RNAscope ISH probing of *Crhr1* and *iCre* mRNA showed strong expression of these molecules within the CeAm (**Figure 2C–G**). Since previous work (e.g., Justice et al., 2008) and our data show that CRF₁⁺ cells are largely localized to the CeAm, analysis of *Crhr1* and *iCre* mRNA expression was focused on this subregion. Quantification of *Crhr1*- and *iCre*-expressing cells within the CeAm showed that more than 90% of *Crhr1*-expressing cells co-express *iCre* (**Figure 2H, I**). There were no significant sex differences in the number of *Crhr1*⁺, *Cre*⁺, and *Crhr1*⁺/*Cre*⁺, but there was a trend for more *Crhr1*⁺ cells in the CeAm of male rats ($p = 0.07$).

Previous work showed that CeA CRF⁺ cells are concentrated in the CeAl, whereas CRF₁⁺ cells are mostly located in the CeAm (Day et al., 1999; Jolkonen and Pitkänen, 1998; Justice et al., 2008; Pomrenze et al., 2015). Immunofluorescent labeling of CRF and ^{td}Tomato protein in the CeA of CRF₁-*Cre-tdTomato* rats shows that the topography of CRF⁺ and ^{td}Tomato⁺ (CRF₁-*Cre*) cells in these rats is consistent with previous studies (**Figure 3**).

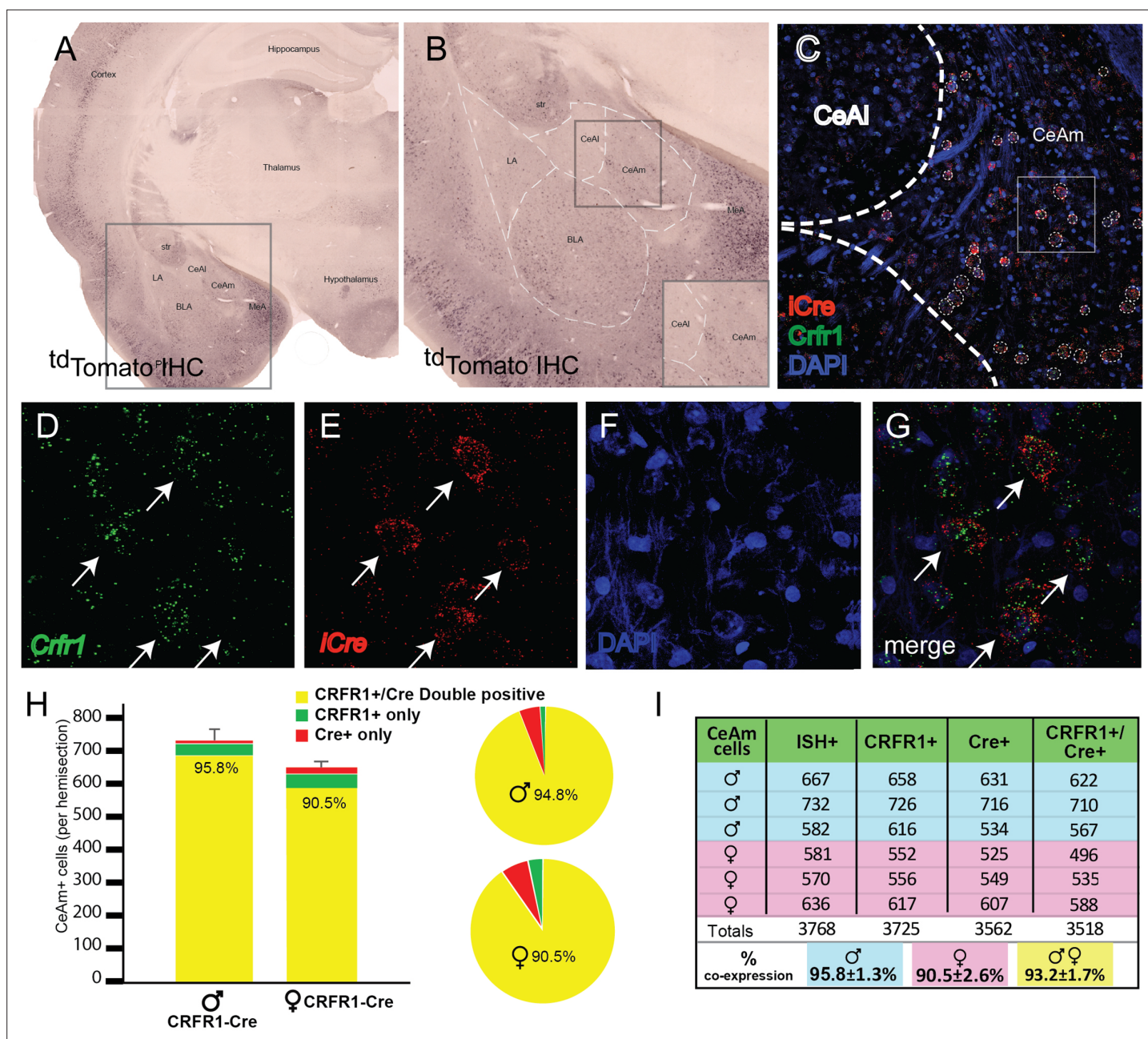


Figure 2. Validation of transgenic expression of $iCre^{tdTomato}$ in CRF_1^+ expressing neurons located in the medial central nucleus of the amygdala (CeAm). (A) A low-magnification image of a section containing the amygdala from a CRF_1 -Cre rat, immunohistochemically labeled for $^{td}Tomato$. Expression of the CRF_1 -Cre transgene is broadly very similar to previous reports of CRF_1 expression in both rat and mouse. (B) Within the boxed region of panel A, higher magnification reveals CRF_1^+ cells in the lateral amygdala (LA), basolateral amygdala (BLA), medial portion central amygdala (CeAm), and medial amygdala (MeA). The lack of significant labeling in the CeAl is consistent with reports using both in situ hybridization and transgenic reporters to detect CRF_1 expression. (C) Micrograph of the CeA from the region boxed in panel B allows visualization of mRNA encoding $iCre$ (red) and $Crhr1$ (green) along with nuclei stained with DAPI (blue). (D–G) Higher magnification images of the boxed region in (C) allows visualization of mRNA for $Crhr1$ (D, green), and $iCre$ (E, red), with nuclei visualized by DAPI staining (F). (G) Merged images reveals that many CeAm neurons that are positive for $Crhr1$ mRNA are also positive for $iCre$ mRNA (arrows point to double positive neurons). Quantification of coincidence of in situ hybridization for both $Crhr1$ and $iCre$ mRNAs demonstrates that >90% of $Crhr1$ -positive cells are also positive for $iCre$ in the CeAm ($n = 3$). (H) Graphical representation of quantification of coincident labeling, or (I) a table of the precise counts from each of three male and three female CRF_1 -Cre transgenic animals. We observed greater than 90% of neurons positive for both $Crhr1$ and $iCre$ in the CeAm.

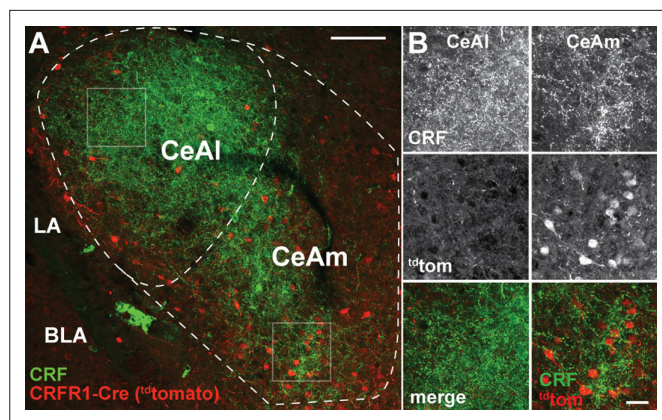


Figure 3. CRF₁-driven expression of Cre/^{td}Tomato in the CeA. **(A)** Visualization of CRF using immunofluorescent labeling (green) in a rat carrying the CRF₁-Cre2aTom transgene (red) reveals minimal cellular expression of CRF₁ in the lateral central nucleus of the amygdala (CeAl) where CRF is highly abundant. This discrepancy in CRF localization compared to CRF₁ expression is consistent with previous reports of CRF₁ expression in both rat and mouse. In contrast to the CeAl, the medial central nucleus of the amygdala (CeAm) contains many CRF₁⁺ neurons (reported by the CRF₁-Cre2aTom transgene), in contact with puncta positive for CRF peptide. **(B)** High-resolution images from the boxed regions of CeAl and CeAm in panel A. CRF staining is dense in both the CeAl and CeAm (top panels); however, cellular expression of the CRF₁-Cre2aTom transgene is low in the CeAl, while many neurons in the CeAm are positive for CRF₁ expression (middle panels). Merged images (lower panels) display the coincident staining of CRF₁⁺ neurons with CRF puncta in the CeAm, suggesting that stress driven CRF release directly signals to CRF₁⁺ neurons in the CeAm to modulate neural excitability to influence the output of CeAm neurons. LA – lateral amygdala, BLA – basolateral amygdala.

Electrophysiological characterization of CeA CRF₁-Cre^{td}Tomato neurons

Membrane properties and inhibitory transmission

^{td}Tomato⁺ CRF₁⁺ neurons were identified and differentiated from unlabeled CeA neurons using fluorescent optics and brief (< 2 s) episcopic illumination in slices from adult male and female CRF₁-Cre^{td}Tomato rats. Consistent with our immunohistochemical studies (**Figure 3**), the majority of CRF₁⁺ neurons were observed in the medial subnucleus of the CeA (CeAm) and this region was targeted for recordings. Passive membrane properties were determined during online voltage-clamp recordings using a 10 mV pulse delivered after break-in and stabilization. The resting membrane potential was determined online after breaking into the cell using the zero current ($I = 0$) recording configuration. No differences were observed between male and female membrane properties including membrane capacitance, membrane resistance, decay time constant, or resting membrane potential (**Figure 4A**). CRF₁⁺ CeA neurons were then placed in current clamp configuration and a depolarizing step protocol was conducted to allow cell-typing based on previously described firing properties (**Chiang et al., 2006; Herman and Roberto, 2016**). The majority of CRF₁⁺ CeA neurons were of the low-threshold bursting type (**Figure 4B**). Voltage-clamp recordings of pharmacologically-isolated GABA_A receptor-mediated spontaneous inhibitory postsynaptic currents (sIPSCs) revealed that CRF₁⁺ neurons are under a significant amount of phasic inhibition (**Figure 4C**) with no significant sex differences in sIPSC frequency (**Figure 4D, left**) or sIPSC amplitude (**Figure 4D, right**). These data indicate that male and female CRF₁⁺ CeA neurons have similar basal membrane properties and are under similar levels of basal inhibitory transmission.

CRF sensitivity

Spontaneous firing activity was recorded in CRF₁⁺ CeA neurons from male and female CRF₁-Cre^{td}Tomato rats using the cell-attached configuration. After a stable baseline period of regular firing was established, CRF (200 nM) was focally applied and the firing activity was recorded for a sustained application period of 7–12 min. CRF₁⁺ CeA neurons from male rats had an average baseline firing rate of 2.1 ± 0.5 Hz and focal application of CRF significantly increased the firing activity to 3.4 ± 0.7 Hz

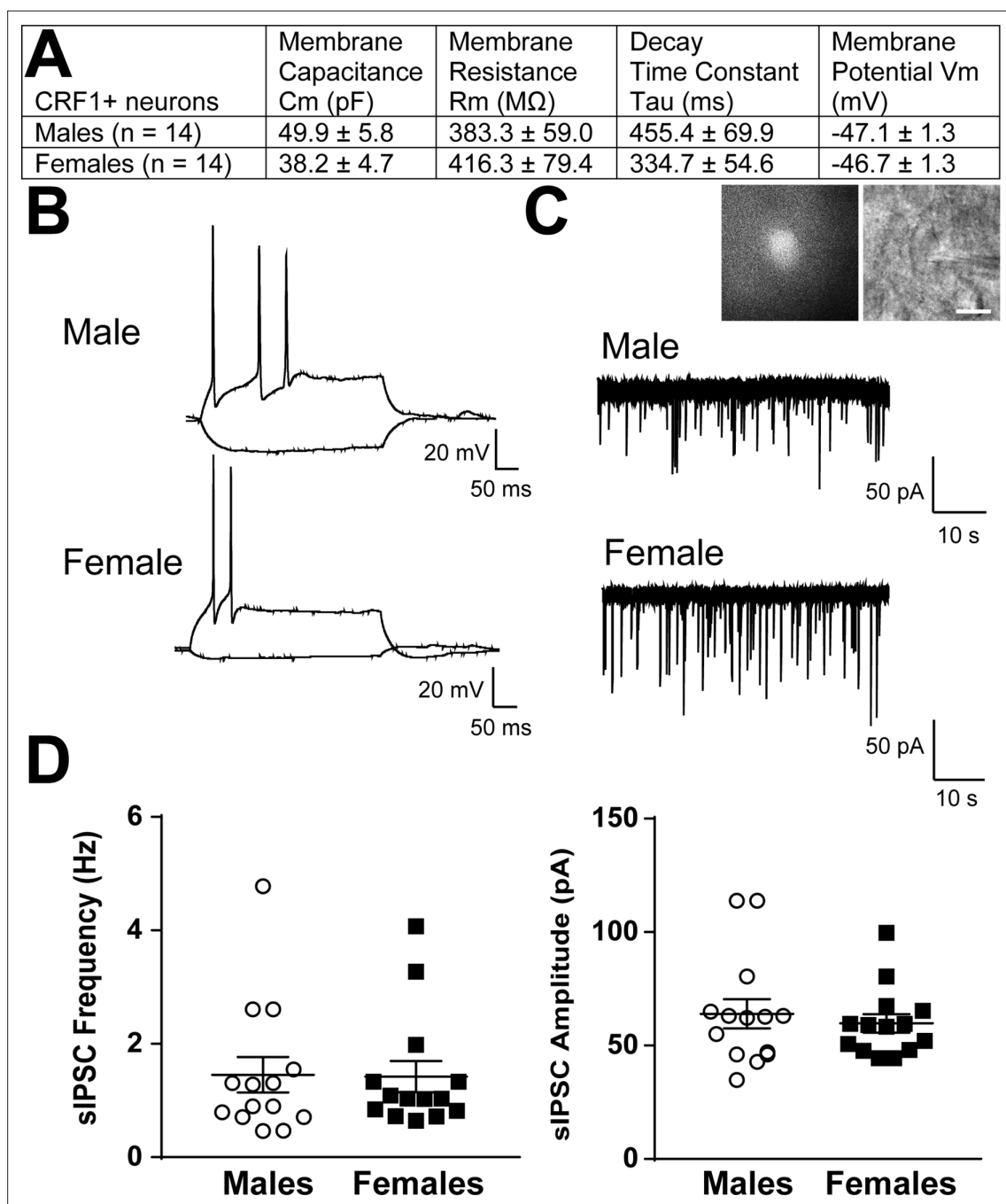


Figure 4. Basal membrane properties and inhibitory synaptic transmission in CeAm CRF₁-Cre^{-td}Tomato neurons. **(A)** Basal membrane properties (Membrane Capacitance, Cm; Membrane Resistance, Rm; Decay Constant, Tau; Membrane Potential, Vm) from male and female CRF₁⁺ CeAm neurons. **(B)** Representative current-evoked spiking properties from male (top) and female (bottom) CRF₁⁺ CeAm neurons. **(C)** Basal spontaneous inhibitory postsynaptic currents (sIPSCs) from male (top) and female (bottom) CRF₁⁺ CeAm neurons (right). *Inset:* representative fluorescent (left) and infrared differential interference contrast (IR-DIC, right) image of a CRF₁⁺ CeAm neuron targeted for recording. Scale bar = 20 μm. **(D)** Average sIPSC frequency (left) and sIPSC amplitude (right) from male and female CRF₁⁺ CeAm neurons. Raw data are available in Source Data File 1.

($t = 3.5$, $p = 0.011$; **Figure 5A and C**). CRF₁⁺ CeA neurons from female rats had an average baseline firing rate of 0.8 ± 0.2 Hz and focal application of CRF significantly increased the firing activity to 1.3 ± 0.3 Hz ($t = 3.1$, $p = 0.016$ by paired t-test; **Figure 5B and D**). When firing activity was normalized to baseline values, CRF application significantly increased firing in CRF₁⁺ CeA neurons from male rats to $192.3\% \pm 25.6\%$ of Control ($t = 3.6$, $p = 0.009$; **Figure 5E**) and significantly increased firing in CRF₁⁺

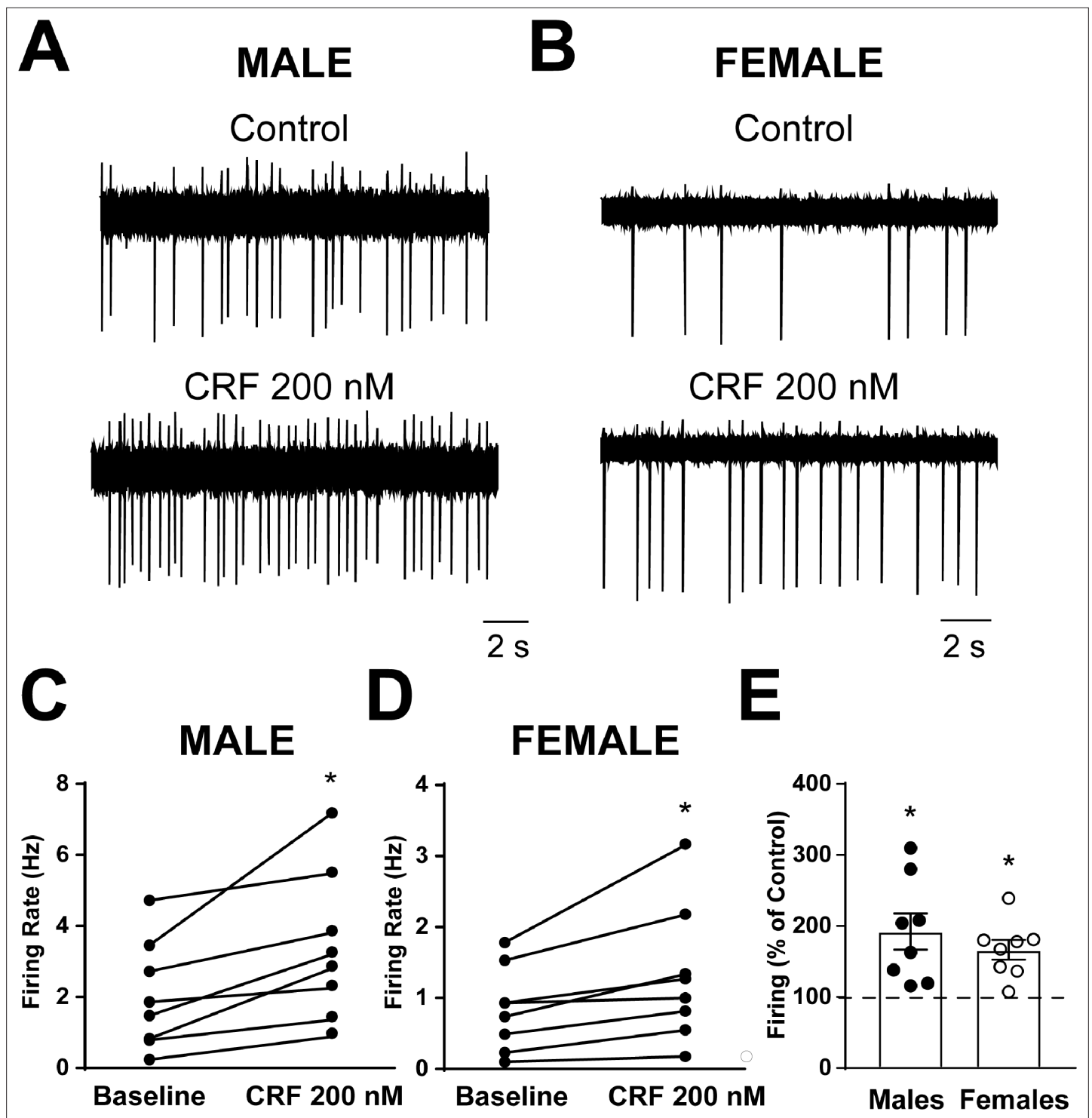


Figure 5. Spontaneous firing activity and CRF sensitivity of CeAm CRF_1 -Cre- td Tomato neurons. **(A)** Representative cell-attached recording of spontaneous firing activity in a CRF_1^+ CeAm neuron from a male CRF_1 -Cre- td Tomato rat before and during CRF (200 nM) application. **(B)** Representative cell-attached recording of spontaneous firing activity in a CRF_1^+ CeAm neuron from a female CRF_1 -Cre- td Tomato rat before and during CRF (200 nM) application. **(C)** Summary of changes in spontaneous firing activity with CRF application in CRF_1^+ CeAm neurons from male CRF_1 -Cre- td Tomato rats. * $p < 0.05$ by paired t-test. **(D)** Summary of changes in spontaneous firing activity with CRF application in CRF_1^+ CeAm neurons from female CRF_1 -Cre- td Tomato rats. * $p < 0.05$ by paired t-test. **(E)** Normalized change in firing activity in CRF_1^+ CeAm neurons from male and female CRF_1 -Cre- td Tomato rats. * $p < 0.05$ by one-sample t-test. Raw data are available in Source Data File 1.

CeA neurons from female rats to $166.5\% \pm 13.9\%$ of Control ($t = 4.8$, $p = 0.002$; **Figure 5E**) with no significant difference in the change in firing in response to CRF between male and female CRF₁⁺ neurons.

Targeting of Cre-dependent Gq-DREADDs to the CeA increases c-Fos⁺ CRF₁-Cre^{-td}Tomato cells and CeA CRF₁-Cre^{-td}Tomato cell activity following CNO treatment *c-Fos immunohistochemistry*: Four weeks after CRF₁-Cre^{-td}Tomato male and female rats were given intra-CeA microinjections of AAV8-hSyn-DIO-HA-hM3D(Gq)-IRES-mCitrine (Active Virus) or AAV5-hSyn-DIO-EGFP (Control Virus), rats were given an injection (i.p.) of CNO (4 mg/kg) and were sacrificed 90 min later. Brain sections containing the CeA were processed for c-Fos immunohistochemistry and the number of c-Fos⁺ tdTomato cells were quantified. An overwhelming majority of tdTomato cells were located in the CeAm as shown above (**Figure 3**). Therefore, quantification of c-Fos and tdTomato cells was focused on this subregion. We found that rats in the active virus group had a higher percentage of c-Fos⁺ tdTomato cells than rats in the control virus group ($t = 7.1$, $p < 0.001$; **Figure 6A and B**).

Slice electrophysiology

Coronal sections containing the CeA were prepared from male and female CRF₁-Cre^{-td}Tomato rats > 4 weeks after rats were given intra-CeA microinjections of AAV8-hSyn-DIO-HA-hM3D(Gq)-IRES-mCitrine. tdTomato⁺ and mCitrine⁺ neurons were identified by brief episcopic illumination using fluorescent optics and positively-identified neurons were targeted for recording in whole-cell current clamp configuration to measure changes in resting membrane potential and spontaneous firing. CNO (10 μM) significantly increased membrane potential and number of action potentials in both male ($t = 4.3$, $p = 0.002$; $t = 2.6$, $p = 0.030$, respectively; **Figure 6C and D**) and in female CRF₁⁺ mCitrine⁺ neurons in the CeA ($t = 3.2$, $p = 0.016$; $t = 3.6$, $p = 0.006$, respectively; **Figure 6E and F**), suggesting that hM3D(Gq) receptor expression was functional and could be stimulated by CNO application with no sex differences in expression or agonist sensitivity.

Chemogenetic stimulation of CeA CRF₁-Cre^{-td}Tomato cells increases mechanical nociception and anxiety-like behaviors

Rats were given intra-CeA microinjections of a viral vector for Cre-dependent expression of Gq-DREADD receptors (AAV8-hSyn-DIO-HA-hM3D(Gq)-IRES-mCitrine) or control fluorophore (AAV5-hSyn-DIO-EGFP) (**Figure 7A**). Behavioral procedures began ≥ 4 weeks later (**Figure 7B**).

Nociception

In the Von Frey test of mechanical nociception, CNO treatment decreased paw withdrawal thresholds in rats that have hM3D(Gq) expression targeted to CeA CRF₁⁺ cells [repeated measures ANOVA; test x treatment interaction ($F_{1,13} = 14.0$, $p = 0.002$)]. There was a significant effect of test within the CNO group only [$(F_{1,7} = 38.0$, $p < 0.001)$], suggesting that chemogenetic stimulation of CeA CRF₁⁺ cells increases mechanical sensitivity. CNO treatment had no effect on paw withdrawal thresholds in rats that received the control EGFP fluorophore (**Figure 7C**). In the Hargreaves test of thermal nociception, CNO did not affect paw withdrawal latencies in either the hM3D(Gq) or control EGFP groups (**Figure 7D**).

Anxiety-like behaviors

In the EPM test, in the hM3D(Gq) group, rats that were given CNO treatment had lower open arms time compared to rats that were given vehicle treatment (t-test; $t = 2.6$, $p = 0.022$), suggesting that chemogenetic stimulation of CeA CRF₁⁺ cells increases anxiety-like behavior on the EPM. Control EGFP virus rats did not show differences in open arms times after CNO treatment (**Figure 7E**). One rat in the hM3D(Gq) group that was given vehicle injection fell off the maze >3 times and was therefore excluded from analysis. In the OF field test, hM3D(Gq) rats that were given CNO treatment spent less time in the center of the arena compared to rats that were given vehicle treatment (t-test; $t = 3.3$, $p = 0.006$), suggesting that chemogenetic stimulation of CeA CRF₁⁺ cells increases anxiety-like behavior in

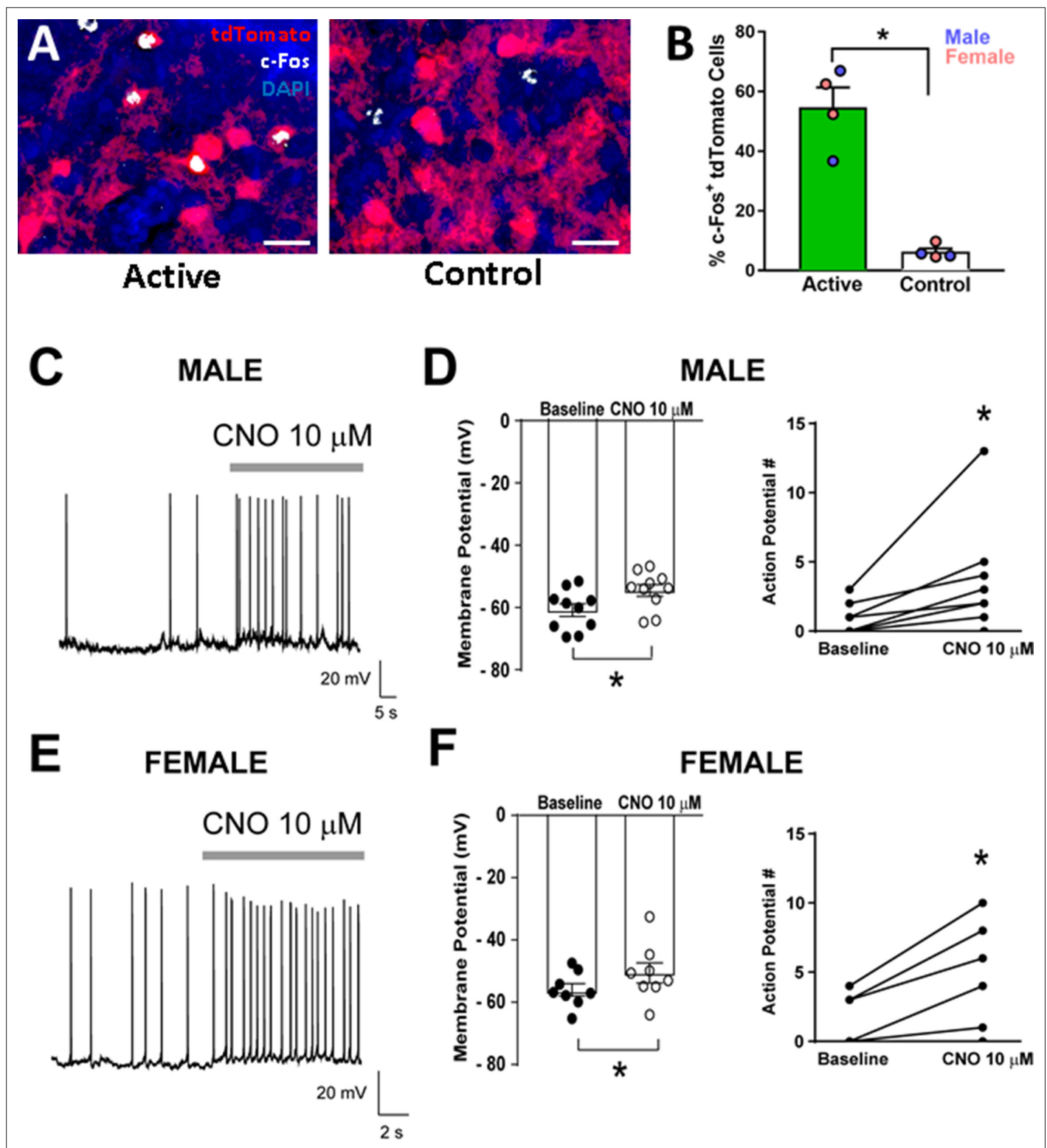


Figure 6. Validation of DREADD expression and function in CeA CRF₁-Cre-^{td}Tomato neurons. (A) Representative images of CRF₁-Cre-^{td}Tomato cells (red) and c-Fos immunostaining (white) in CeAm of rats that were given intra-CeA microinjections of AAV8-hSyn-DIO-HA-hM3D(Gq)-IRES-mCitrine (active virus) or AAV5-hSyn-DIO-EGFP (control virus). Scale bar: 50 μm. (B) CNO treatment 90 min before sacrifice increased the percentage of c-Fos⁺ ^{td}Tomato cells in CeAm of rats that were given active virus compared to rats that were given control virus microinjections. *p < 0.05. (C) Representative whole-cell current clamp recording of membrane potential and firing activity in a CRF₁⁺ CeAm neuron from a male CRF₁-Cre-^{td}Tomato rat before and during CNO (10 μM) application. (D) Summary of the change in membrane potential (left) and action potentials (right) in male CRF₁⁺ CeAm neurons after CNO

Figure 6 continued on next page

Figure 6 continued

application. * $p < 0.05$ by paired t-test. (E) Representative whole-cell current clamp recording of membrane potential and firing activity in a CRF_1^+ CeAm neuron from a female CRF_1 -Cre- td Tomato rat before and during CNO (10 μ M) application. (D) Summary of the change in membrane potential (left) and action potentials (right) in female CRF_1^+ CeAm neurons after CNO application. * $p < 0.05$ by paired t-test. Raw data are available in Source Data File 1.

the OF. EGFP control rats did not show differences in time spent in the center of the arena after CNO treatment (Figure 7F). In the LD test, CNO treatment did not produce differences in time spent in the light box in either hM3D(Gq) or EGFP control groups (Figure 7G). There were also no differences in latency to enter the light box (data not shown; 20.14 ± 5.63 s, 29.38 ± 10.42 s, 23.00 ± 3.94 s, and 16.17 ± 4.48 s, respectively, for rats in hM3D(Gq) – Veh, hM3D(Gq) – CNO, EGFP – Veh, and EGFP Virus – CNO groups).

Given that most cells in the CeA are GABAergic, we next tested if *Crhr1* and *iCre* mRNA are also highly colocalized in the BLA, which contains a high density of glutamatergic neurons that express CRF_1 receptors. RNAscope ISH of brain sections containing BLA show dense *Crhr1* and *iCre* mRNA expression in BLA and surrounding areas (Figure 8A). Quantification of *Crhr1* and *iCre* mRNA in the BLA showed that 98.5% of *Crhr1*-expressing cells co-express *iCre* (Figure 8B, top), and that 99.4% of *iCre*-expressing cells co-express *Crhr1* (Figure 8B, bottom).

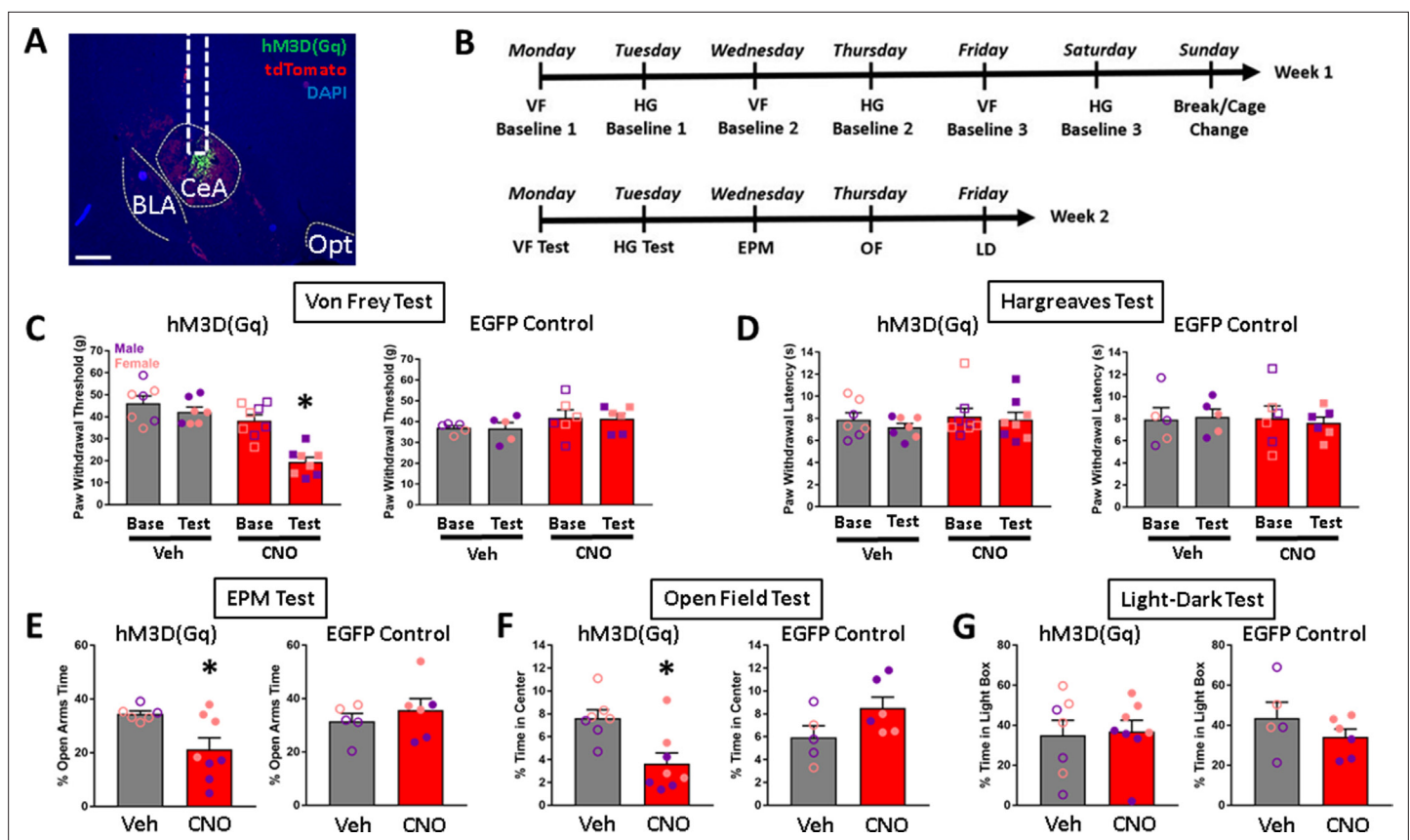


Figure 7. Effects of chemogenetic stimulation of CeA CRF_1 -Cre- td Tomato neurons on nociception and anxiety-like behaviors. (A) Representative image of AAV8-hSyn-DIO-HA-hM3D(Gq)-IRES-mCitrine expression (green) in the CeA. Scale bar: 500 μ m. BLA: basolateral amygdala, Opt: optic tract. (B) Timeline of experimental procedures. (C) CNO treatment decreased paw withdrawal thresholds in the Von Frey test of mechanical nociception in rats that were given intra-CeA hM3D(Gq) virus microinjections. There were no effects of treatment on paw withdrawal thresholds in the EGFP control group. (D) CNO treatment had no effects on paw withdrawal latencies in either the hM3D(Gq) or EGFP groups in the Hargreaves test of thermal nociception. (E) CNO treatment decreased the percent time spent in open arms in the EPM test in the hM3D(Gq) group, but had no effect in the EGFP group. (F) CNO treatment decreased the percent time spent in the center of the arena in the OF test in the hM3D(Gq) group, but had no effect in the EGFP group. (G) CNO treatment had no effect on percent time spent in the light box in the LD test. * $p < 0.05$. Raw data are available in Source Data File 2. *iCre* and *Crhr1* mRNA are highly co-expressed in BLA.

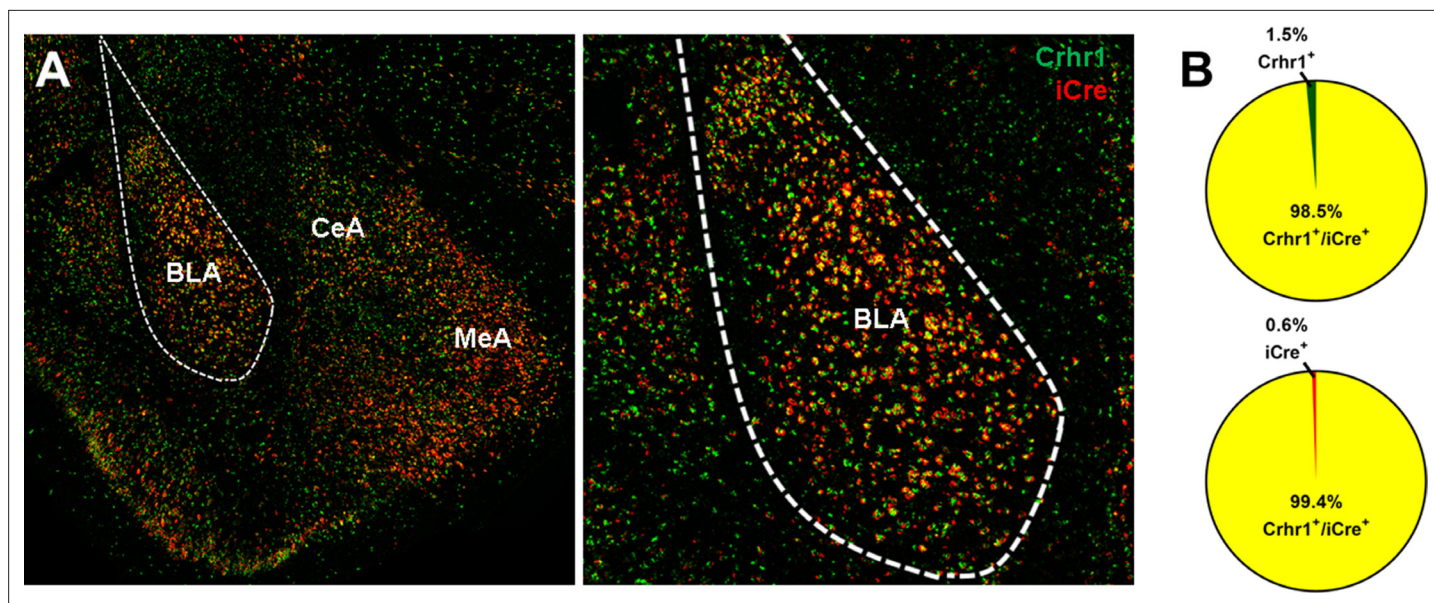


Figure 8. *Crhr1* and *iCre* mRNA expression in BLA of CRF₁-Cre-^{td}Tomato rats. (A) *Crhr1* (green) and *iCre* (red) mRNA are highly co-expressed in BLA and surrounding areas. (B) Within the BLA, 98.5% of *Crhr1*⁺ + co-express *iCre* (top), and 99.4% of *iCre*⁺ + co-express *Crhr1* (bottom).

Cre-^{td}Tomato cells are found throughout the brain in areas known to contain CRF₁ cells

The purpose of this experiment is to examine if the Cre-^{td}Tomato transgene is expressed in brain areas outside of the amygdala in a pattern that is consistent with known CRF₁ expression patterns. Fluorescence imaging of coronal sections across the rostrocaudal axis of CRF₁-Cre-^{td}Tomato rat brains show that Cre-^{td}Tomato cells are found in brain areas known to contain CRF₁ cells, including the prelimbic and infralimbic cortex, BNST, piriform cortex (PIR), PVN, lateral hypothalamus (LHA), paraventricular thalamus (PVT), hippocampus, ventral tegmental area (VTA), periaqueductal grey (PAG), and dorsal raphe (DR) (Figure 9). The density of Cre-^{td}Tomato cells in these brain areas were surveyed and compared to published reports of *Crhr1* mRNA expression patterns in the wildtype rat brain (Van Pett et al., 2000) and of CRF₁-GFP cell densities in CRF₁-GFP mouse brain (Justice et al., 2008; Table 1). We found that a majority of cells in the BNST and PIR, that a substantial number of cells in the PrL, IL, PVT, VTA, PAG, and DR, and that some cells in the ventral lateral septum (LSv), PVN, LHA, and hippocampus are ^{td}Tomato⁺. The lateral (LHb) and medial habenula (MHb) were largely devoid of ^{td}Tomato⁺ cells, but a small number of ^{td}Tomato cells were found in the ventricular zone of the MHb (Figure 9Q). The locus coeruleus (LC) was devoid of ^{td}Tomato cells, but a small number of ^{td}Tomato puncta was detected (Figure 9X). These ^{td}Tomato expression patterns are mostly consistent with *Crhr1* mRNA expression patterns in wildtype rats, but some species-specific differences are seen when compared to GFP expression patterns in CRF₁-GFP mice. Please see Table 1.

Discussion

We generated a new transgenic CRF₁-Cre-^{td}Tomato rat line to allow genetic manipulation and visualization of neurons that express CRF₁ receptors in the rat brain. We report that, within the CeA of CRF₁-Cre-^{td}Tomato rats, CRF₁-Cre-^{td}Tomato cells are located in the medial subdivision (CeAm), consistent with previous reports of *Crhr1* expression in rats (Potter et al., 1994; Van Pett et al., 2000; Day et al., 1999) and mice (Van Pett et al., 2000; Justice et al., 2008), and that there is strong concordance (> 90%) between *Crhr1* and *iCre* mRNA expression in the CeAm of male and female CRF₁-Cre-^{td}Tomato rats. We also characterized the basal membrane properties, inhibitory synaptic transmission, and validated the CRF sensitivity of ^{td}Tomato-expressing CeA CRF₁⁺ cells in male and female rats. In addition, we showed that stimulatory DREADD receptors [hM3D(Gq)] can be targeted to CeA CRF₁-Cre-^{td}Tomato cells using a Cre-dependent expression strategy, that systemic CNO treatment

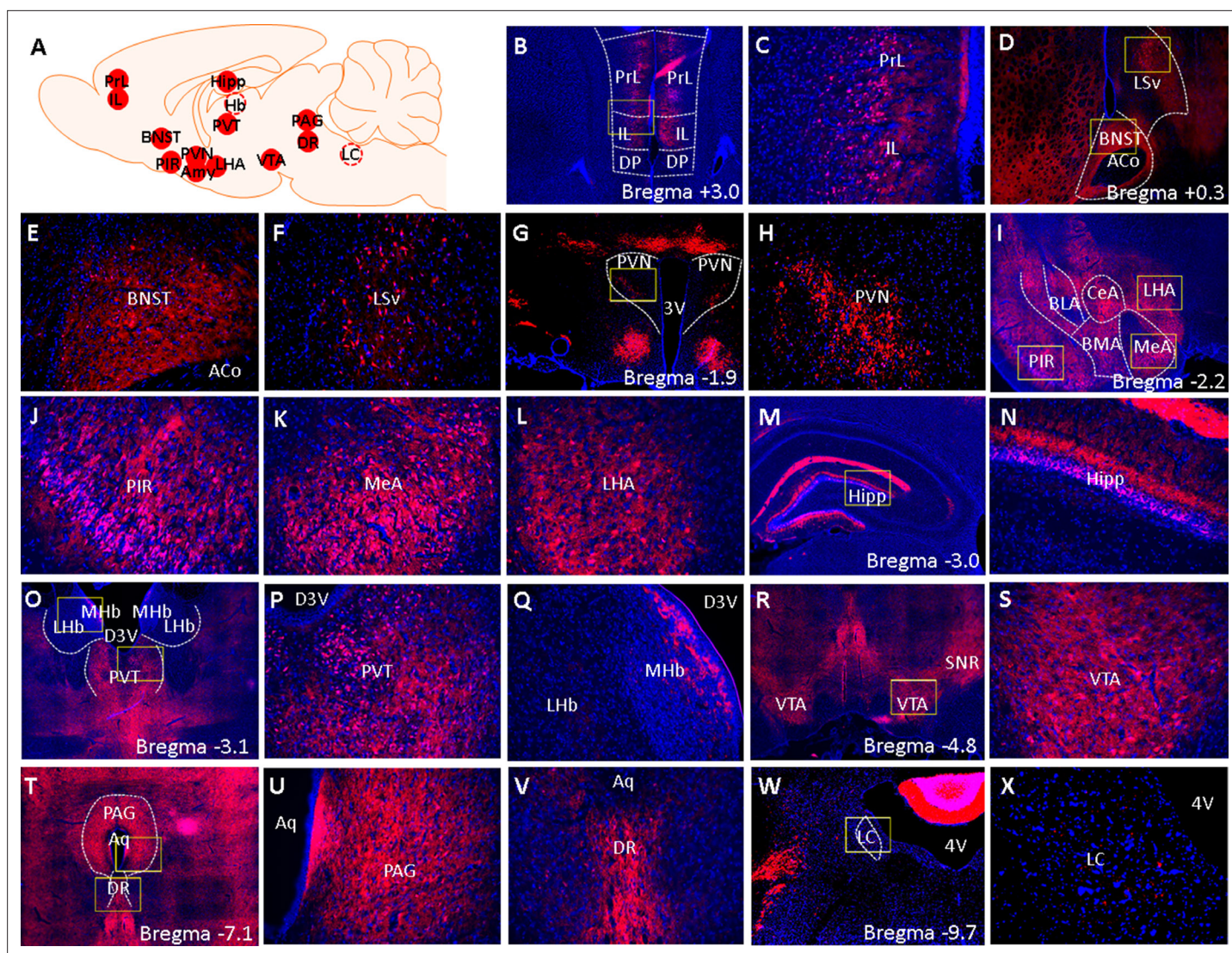


Figure 9. Fluorescent images of brainwide ^{td}Tomato expression. **(A)** A schematic summary of brain areas that were surveyed for tdTomato expression. Solid red circles indicate brain areas that contain ^{td}Tomato cells and dashed circles indicate brain areas that were devoid of ^{td}Tomato cells. **(B–X)** Low (4 x) and high-magnification (x20) images of tdTomato (red) and DAPI (blue) fluorescent signals. Yellow boxes demarcate areas from which high-magnification (x20) images were acquired. **(B)** 4 x image of the PrL, IL, and surrounding landmarks. **(C)** 20 x image of PrL and IL. **(D)** 4 x of BNST and LSV. **(E)** 20 x image of BNST and **(F)** LSV. **(G)** 4 x and **(H)** 20 x image of PVN. **(I)** 4 x image of PIR, MeA, and LHA. **(J)** 20 x image of PIR, **(K)** MeA, and **(L)** LHA. **(M)** 4 x and **(N)** 20 x image of hippocampus. **(O)** 4 x image PVT, LHB, and MHb. **(P)** 20 x image of PVT and **(Q)** LHB/MHb. **(R)** 4 x and **(S)** 20 x image of VTA. **(T)** 4 x image of PAG and DR. **(U)** 20 x image of PAG and **(V)** DR. **(W)** 4 x and **(X)** 20 x image of LC. 3 V: 3rd ventricle, 4 V: 4th ventricle, D3V: dorsal 3rd ventricle, Aq: cerebral aqueduct.

induces c-Fos in hM3D(Gq)-transduced CRF₁⁺ cells in CeA, and that CNO induces membrane depolarization and spontaneous firing activity in hM3D(Gq)-transduced CRF₁⁺ cells in CeA. We showed that hM3D(Gq)-mediated stimulation of CeA CRF₁⁺ cells increases anxiety-like behavior, as measured by EPM and open field tests, as well as mechanical nociception as measured by the Von Frey test. Finally, we report that *Crhr1* and *iCre* mRNA expression are highly colocalized in the BLA, and that Cre-^{td}Tomato is expressed in several brain areas across the rostrocaudal axis of the rat brain in expected patterns. Collectively, this work provides cellular, electrophysiological, and behavioral data demonstrating the validity and reliability of a new transgenic rat model for the identification and selective manipulation of CRF₁⁺ neurons in the CeA.

CRF₁-Cre-^{td}Tomato rats were generated by modifying a BAC clone derived from F344 rats, that was injected into oocytes derived from Wistar rats. Because the originating strain of the BAC DNA differs

Table 1. Comparison of CRF₁-Cre-tdTomato cell densities with *Crhr1* mRNA expression levels in rats and CRF₁-GFP cell densities in mice in several areas across the rostrocaudal axis of the brain.

+: Some cells are positive, ++: A substantial number of cells are positive, +++: Most cells are positive.

Brain area	Density of tdTomato cells in CRF ₁ -Cre-tdTomato rats	Expression level of <i>Crhr1</i> mRNA in wildtype rats (Van Pett et al., 2000)	Density of GFP cells in CRF ₁ -GFP Mice (Justice et al., 2008)
PrL	++	++	++
IL	++	++	++
BNST	+++	+++	+ / ++
LSv	+	+	-
PVN	+	+	++
PIR	+++	+++	+ / +++
MeA	++	+	+ / ++
LHA	+	+	++
Hipp	+ (subiculum, CA3) / +++ (CA1)	++ (CA1, CA3, subiculum)	+ (subiculum, CA3) / +++ (CA1)
PVT	++	++	-
LHb	-	-	++
MHb	+	-	-
VTA	++	++	++
PAG	++	+	+
DR	++	+	++
LC	-	-	+ / -

from the strain used for transgenesis, DNA sequence differences between F344 and Wistar rats in the 200 + kb region surrounding the *Crhr1* genomic locus may impact expression of iCre-2A-tdTomato in the CRF₁-Cre transgenic rat. Moreover, because transgenic BAC DNA insertion was not directed, position effect, copy number, and fragmentation of the BAC insertion may possibly alter expression of reporter genes. These sources of variability were minimized by the expertise of the UNC Transgenic Core Facility, where BAC DNA was prepared, cleaved at a single site to produce full-length single stranded BAC DNA, then injected into oocytes. Two transgenic founders were isolated that contained unique DNA sequences near the *Crhr1* genomic locus in the BAC, as well as DNA sequence from both terminal ends of the injected BAC, indicating insertion of full-length BAC DNA. Of these two rats, one displayed expression of tdTomato in a pattern reflecting *Crhr1* expression patterns reported in rats (Potter et al., 1994; Van Pett et al., 2000), as well as transgenic expression of reporter genes reported in similarly designed BAC transgenic mice (Justice et al., 2008; Jiang et al., 2018; Hunt et al., 2018). The genomic locus and copy number of transgenic BAC insertion have not been further characterized. However, the high degree of alignment of Cre-tdTomato expression with known CRF₁ expression patterns broadly throughout the brain suggests that position, copy number, or fragmentation did not substantially alter expression of the transgene. In addition, the behavioral and physiological phenotypes of CRF₁-Cre-tdTomato rats reported here closely resemble those seen in wild-type Wistar rats (e.g., Itoga et al., 2016; Albrechet-Souza et al., 2020; see below), suggesting that BAC insertion did not produce observable anomalous phenotypes.

The intrinsic properties of CRF₁⁺ (tdTomato⁺) CeA neurons in CRF₁-Cre-tdTomato rats are similar to those reported in wild-type rat CeA neurons (Herman and Roberto, 2016), suggesting that the transgene did not significantly impact the overall health or activity of CRF₁⁺ CeA neurons. Previous studies have employed a CRFR1:GFP transgenic mouse model to examine CRF₁⁺ CeA neurons in local CeA microcircuitry (Herman et al., 2013; Herman et al., 2016). Although prior work was conducted in mouse and some species differences would be expected, the electrophysiological properties of CRF₁⁺ neurons in the CeA are relatively consistent between the mouse and rat transgenic models. Recent work specifically examining sex differences in CRF₁⁺ neurons from CRFR1:GFP mice reported similar

intrinsic membrane properties, cell-typing, and baseline inhibitory transmission as reported here and noted no sex differences in basal properties between male and female CRF₁⁺ neurons in the CeA (**Agoglia et al., 2020**), consistent with our current findings. In contrast to previous work, however, we found no sex differences in CRF sensitivity of CRF₁⁺ cells in CeA. Although CRF was previously found to increase firing in CRF₁⁺ CeA neurons in both male and female mice, CRF₁⁺ CeA neurons from male mice displayed a significantly greater increase in firing in response to CRF application (**Agoglia et al., 2020**). This discrepancy may be driven by differences in sampling size (although the current study was not sufficiently powered to detect sex differences), high variability in male baseline firing rates observed here, sex differences in baseline firing rates observed here, or it may reflect a species difference in sex-dependent sensitivity to CRF. Additional studies are required for a more comprehensive examination of sex- and/or species-specific differences in CRF-stimulated CRF₁⁺ neuronal activity in distinct brain regions. CRF₁⁺ neurons in the CeA have also previously been implicated in the neuroplastic changes associated with acute and chronic ethanol exposure in mice (**Herman et al., 2013; Herman et al., 2016**), and future work will determine if this is also the case in rats.

To test the feasibility of using Cre-dependent stimulatory DREADDs to interrogate the role of CeA CRF₁⁺ cells in behavior, we targeted Gq-coupled DREADD receptors [DIO-hM3D(Gq)] to CeA CRF₁-Cre cells and first tested the effects of CeA CRF₁⁺ cell stimulation on nociception. We showed that DREADD stimulation of CeA CRF₁⁺ cells increases mechanical sensitivity as measured by the Von Frey test, but not thermal sensitivity measured by the Hargreaves test. Numerous studies have implicated CeA CRF-CRF₁ signaling in nociception. For instance, pain induced by carrageenan injection into the knee joint produces hyperactivity of CeA neurons in rats, a phenomenon that is CRF₁ dependent (**Ji and Neugebauer, 2007**). Conversely, latency for hind limb withdrawal reflex induced by knee joint pressure application is decreased (reflecting hyperalgesia) by CRF infusion into the CeA, a phenomenon that is blocked by co-infusion of a CRF₁ antagonist (**Ji et al., 2013**). With regard to mechanical sensitivity, our finding that DREADD activation of CeA CRF₁ neurons produces mechanical hypersensitivity extends previous work showing that ablation or inhibition of CeA CRF neurons blocks neuropathic pain-induced mechanical hypersensitivity, as measured by the Von Frey test (**Andreoli et al., 2017**). Various studies have also previously reported that CeA CRF₁ antagonism attenuates mechanical hypersensitivity produced by chronic drug or alcohol exposure (e.g. **Cohen et al., 2015; Edwards et al., 2012**). Collectively, this prior work suggests that activation of CeA CRF-CRF₁ signaling by chronic injuries or insults facilitates a hyperalgesic state, which was recapitulated in the current study via chemogenetic stimulation of CeA CRF₁ cells. It should be noted that chemogenetic stimulation of CeA CRF⁺ cells has been shown to potentiate stress-induced analgesia (**Andreoli et al., 2017**), although this effect may be due to CRF release outside the CeA (e.g. locus coeruleus) or due to changes in GABA release from CRF⁺ cells. Within the CeA, pharmacological studies suggest that pro- and anti-nociceptive effects of CRF signaling may be mediated by CRF₁ and CRF₂ receptors, respectively (**Ji and Neugebauer, 2007; Ji and Neugebauer, 2008**), but further studies are required to delineate the precise mechanisms by which CeA CRF signaling supports hyperalgesia and analgesia. The CRF₁-Cre^{-tdTomato} rat described here represents a useful tool for these studies.

Our lab has shown that predator odor stress-induced hyperalgesia, as measured by the Hargreaves test, is mediated by increased CRF-CRF₁ signaling in the CeA (**Itoga et al., 2016**). Contrary to our hypothesis, we did not observe any effect of DREADD activation of CeA CRF₁ cells on thermal sensitivity. It is not clear why CRF₁-Cre rats exhibited mechanical hypersensitivity but not thermal hyperalgesia in this study. It is possible that specific CeA cell populations are involved in specific types of nociceptive processing, or it is possible that the engagement/recruitment of CeA CRF₁⁺ cells in mediating specific types of nociception depends on the animal's history or affective state. Using the CRF₁-Cre^{-tdTomato} rat line reported here, future work will elucidate the role of specific CRF₁⁺ circuits in mechanical and thermal sensitivity (which may or may not be partially overlapping) under basal and challenged conditions such as neuropathic or inflammatory pain, stress exposure and/or withdrawal from chronic exposure to drugs or alcohol.

CeA CRF-CRF₁ signaling generally promotes anxiogenic responses, particularly under challenged conditions such as stress or withdrawal from chronic exposure to drugs of abuse. For instance, in mice, intra-CeA infusion of a CRF₁ antagonist attenuates anxiety-like behavior, as measured by open field and light-dark box tests, following immobilization stress but not under basal conditions (**Henry et al., 2006**). Similarly, blockade of CRF-CRF₁ signaling in the CeA attenuates alcohol withdrawal-induced

anxiety in rats, as measured by the EPM test (*Rassnick et al., 1993*). Exposure to stressors (*Merlo Pich et al., 1995*) and alcohol withdrawal (*Zorrilla et al., 2001*) both increase extracellular CRF levels in the CeA. Messing and colleagues used CRF-Cre rats to show that CeA CRF cell activation (using DREADDs) increases anxiety-like behavior and that this effect is blocked by CeA CRF knockdown using RNA interference (*Pomrenze et al., 2019*). Collectively, these studies show that increased CRF-CRF₁ signaling in CeA, whether produced by stress exposure, drug withdrawal, or the use of viral genetic tools, supports anxiogenesis. Here, we showed that chemogenetic stimulation of CeA CRF₁⁺ cells increases anxiety-like behavior, as measured by EPM and open field tests. Interestingly, we did not observe an effect of chemogenetic stimulation of CeA CRF₁⁺ cells on light-dark box measures, including time spent in the light vs. dark boxes, latency to enter light box, and number of crosses between the two compartments. Previous studies reported that the light-dark box test may be more suited for detecting anxiolytic rather than anxiogenic effects (*Crawley and Davis, 1982*), and that animals' responses in this test is affected by the intensity of illumination in the animal's regular housing room (*File et al., 2004*). Future studies will test if Cre-dependent expression of inhibitory chemogenetic or optogenetic strategies can be applied to inhibit CeA CRF₁ cells, and if inhibition of CeA CRF₁ cells reduces anxiety-like behavior at baseline or after stress exposure.

Although the CeA is generally not thought to exhibit strong sexual dimorphism, sex differences have been reported for CRF and CRF₁ properties in the CeA. For example, female rats in proestrus have higher levels of CeA *Crf* mRNA than male rats and footshock stress induces greater CeA *Crf* expression in female proestrus than in male rats (*Iwasaki-Sekino et al., 2009*). However, using autoradiography, Cooke and colleagues reported no sex differences in CRF₁ receptor binding in the CeA of rats (*Weathington et al., 2014*). Using a transgenic CRFR1:GFP mouse line, the CeA of male animals was shown to contain more CRF₁⁺ cells than female animals (*Agoglia et al., 2020*). In the current study, although underpowered to detect sex effects, we found that male CRF₁-Cre-^{td}Tomato rats tend to have more CRF₁⁺ cells within the CeA than female rats, as detected via RNAscope in situ hybridization. Previous work using CRFR1:GFP mice (*Agoglia et al., 2020*) and our current work using CRF₁-Cre-^{td}Tomato rats revealed no sex differences in basal membrane properties and inhibitory synaptic transmission in CeA CRF₁⁺ neurons. Our previous work in CRFR1:GFP mice showed that, while CRF application increased firing in CRF₁⁺ CeA neurons from both female and male mice, larger increases were observed in CRF₁⁺ neurons from male mice, an effect that we did not observe in rats potentially due to differences in variability or sex differences in firing rate.

The overwhelming majority of published studies examining the role of CeA CRF₁ signaling in nociceptive and anxiety-like behaviors has employed only male subjects. Here, we used both sexes in tests of nociception and anxiety-like behavior and we did not detect any sex differences. However, we observed that the anxiogenic effect of CeA CRF₁⁺ cell activation in the EPM test was driven by stronger effects in male subjects. One interpretation is that CeA CRF₁⁺ cell activation affects specific components of anxiety-related behavior, that these components are aligned with specific 'anxiety-like behavior' phenotypes in male versus female rats that are more or less detectable by these various tests. In support of this idea, a meta-analysis of studies of anxiety-like behavior in rats and mice revealed a discordance in results between the EPM and open field tests (*Mohammad et al., 2016*). However, due to the small number of studies testing female animals, the role of sex in this discordance is still unknown. Within the EPM literature, studies have shown that the EPM test is more reliable for detecting anxiogenic effects in male rather than female rodents (e.g. *Scholl et al., 2019*). Collectively, these findings demonstrate the importance of behavioral assay selection and of using both male and female subjects.

In summary, we present a novel CRF₁-Cre-^{td}Tomato rat line that allows for the visualization and manipulation of CRF₁-expressing cells. The CRF₁-Cre rat can be used to study the role of distinct CRF₁⁺ cell populations and circuits in physiology and behavior. In addition, the expression of the fluorescent reporter ^{td}Tomato in CRF₁-expressing cells will allow for high resolution, detailed analysis of the expression pattern of CRF₁ that has not been possible due to the lack of CRF₁-specific antibodies.

Materials and methods

Key resources table

Reagent type (species) or resource	Designation	Source or reference	Identifiers	Additional information
Gene (<i>Rattus norvegicus</i>)	BAC containing the <i>Crf1</i> genomic locus	Riken Gene Engineering Division	RNB2-336H12	
Transfected construct (<i>Rattus norvegicus</i>)	<i>iCre-2a-tdTomato</i> BAC transgene	This paper		See Results, Design of CRF ₁ -Cre BAC; Contact Justice Lab
Genetic reagent (<i>Rattus norvegicus</i>)	CRF ₁ -Cre- ^{td} Tomato rat	This paper		See Results, Generation of Transgenic Rats; Contact Gilpin Lab
Recombinant DNA reagent	AAV8-hSyn-DIO-HA-hM3D(Gq)-IRES-mCitrine	Addgene	Cat# 50454-AAV8	
Recombinant DNA reagent	AAV5-hSyn-DIO-EGFP	Addgene	Cat# 50457-AAV5	
Antibody	Anti-c-Fos (Rabbit polyclonal)	Abcam	Cat# ab190289, RRID:AB_2737414	(1:1000)
Antibody	Anti-HA-Tag (Rabbit monoclonal)	Cell Signaling	Cat# 3724, RRID:AB_1549585	(1:250)
Antibody	Anti-RFP (Rabbit monoclonal)	Abcam	Cat# ab34771, RRID:AB_777699	(1:500)
Antibody	Anti-CRF (Rabbit monoclonal)	The Salk Institute	Rc-68	(1:2000)
Commercial assay or kit	RNAscope Multiplex Fluorescent Kit v2	ACD Bio	<i>iCre</i> and <i>Crf1</i> probes	
Commercial assay or kit	TSA Detection Kit	Akoya Biosciences	Cat# NEL701A001KT	
Commercial assay or kit	Prolong Gold Antifade Reagent with DAPI	Invitrogen	Cat# P36935	
Chemical compound, drug	Clozapine-n-oxide	NIH Drug Supply Program		
Chemical compound, drug	Corticotropin-releasing factor	Tocris	Cat# 1,607	
Software, algorithm	Mini Analysis	Synaptosoft Inc.	RRID:SCR_002184	
Software, algorithm	Clampfit 10.6	Molecular Devices		
Software, algorithm	Prism 7.0	GraphPad	RRID:SCR_002798	
Software, algorithm	SPSS 25	IBM SPSS	RRID:SCR_019096	

Subjects

Adult male and female CRF₁-Cre-^{td}Tomato rats were used in all experiments. Rats bred from the original founder F1 line were group-housed in humidity- and temperature-controlled (22 °C) vivaria at UNC, LSUHSC, or UTHSC on a reverse 12 hr light/dark cycle (lights off at 7:00 or 8:00 AM) and had ad libitum access to food and water. All behavioral procedures occurred in the dark phase of the light-dark cycle. Sample sizes were estimated using published work from our labs. In situ hybridization and immunohistochemistry experiments were performed in a single pass. Behavioral experiments were performed in two independent, fully counterbalanced replicates. Slice electrophysiology experiments were conducted in a single pass, such that one experiment was performed in each slice and each experimental group contained neurons from a minimum of three rats. All procedures were approved by the Institutional Animal Care and Use Committee of the respective institutions at which procedures occurred (LSUHSC IACUC Protocol #3749; UNC IACUC Protocol #19–190; UTHSC IACUC Protocol #21–075) and were in accordance with National Institutes of Health guidelines.

Stereotaxic surgeries

Rats were anesthetized with isoflurane (2 min at 4% for induction, 1%–3% for maintenance) and mounted into a stereotaxic frame (Kopf Instruments) for all stereotaxic surgeries. The following coordinates (from bregma) were used for bilateral intra-CeA microinjections: –2.5 mm posterior, ± 4.0 mm lateral, and –8.4 mm ventral for male rats and –2.2 mm posterior, ± 4.0 mm lateral, and –8.2 mm ventral for female rats. Viral vectors for Cre-dependent expression of Gq-DREADDs or control (see below) were injected into each side of the CeA at a volume of 0.5 µL over 5 min and injectors were

left in place for an additional 2 min. Viral titers were between $1.0\text{--}1.5 \times 10^{13}$ GC/mL. At the end of surgeries, rats were monitored to ensure recovery from anesthesia and were given a minimum of 4 weeks to recover before the start of procedures. Rats were treated with the analgesic flunixin (2.5 mg/kg, s.c.) and, in some rats, the antibiotic cefazolin (20 mg/kg, i.m.) before the start of surgeries and once the following day.

Immunohistochemistry

Rats were deeply anesthetized with isoflurane and were transcardially perfused with ice-cold phosphate buffered saline (PBS) followed by 4% paraformaldehyde (PFA). Brains were extracted and post-fixed in 4% PFA for 24 hr (at 4 °C), cryoprotected in 20% sucrose for 48–72 hr (at 4 °C), and frozen in 2-methylbutane on dry ice. Coronal sections were collected using a cryostat and stored in 0.1% sodium azide in PBS at 4 °C until further processing.

c-Fos immunofluorescent labeling

Sections (40 μm) containing the CeA were washed 3×10 min in PBS and incubated in blocking buffer (2.5% normal goat serum with 0.3% Triton X-100) for 2 hr at RT. Subsequently, sections were incubated in rabbit anti-c-Fos polyclonal antibody (1:1000 in blocking buffer; catalog no. 190289, Abcam, Cambridge, United Kingdom) for 48 hr at 4 °C. Sections were then washed 3×10 min in PBS and incubated in goat anti-rabbit Alexa Fluor 647 (1:500 in blocking buffer; catalog no. A32733, Invitrogen, Carlsbad, CA) for 2 hr at RT. After 3×10 min washes in PBS, sections were mounted on microscope slides and coverslipped with Prolong Gold Antifade Reagent with DAPI (Invitrogen, catalog no. P36935). Sections were imaged using a Keyence (Osaka, Japan) BZ-X800 fluorescent microscope at $\times 20$ magnification and Fos⁺ cells were quantified manually by a blinded experimenter. Four sections representative of the CeA anterior-posterior axis (\sim bregma $-1.8\text{--}2.8$) from each animal were used for analysis.

HA-tag immunofluorescent labeling

Sections (40 μm) containing the CeA were washed 3×10 min in PBS and incubated in 3% hydrogen peroxide for 5 min. Sections were then washed 3×10 min in PBS and incubated in a blocking buffer containing 1% (w/v) bovine serum albumin and 0.3% Triton X-100 in PBS for 1 h at room temperature (RT). Then, sections were incubated in a rabbit anti-HA monoclonal antibody (1:250 in blocking buffer; catalog no. 3724, Cell Signaling, Danvers, MA) for 48 hr at 4 °C. Sections were then washed for 10 min in TNT buffer (0.1 M Tris base in saline with 0.3% Triton X-100), incubated for 30 min in 0.5% (w/v) Tyramide Signal Amplification (TSA) blocking reagent in 0.1 M Tris base, and incubated for 30 min in ImmPRESS horseradish peroxidase horse anti-rabbit antibody (catalog no. MP-7401, Vector Laboratories, Burlingame, CA) at RT. Following 4×5 min washes in TNT buffer, sections were incubated in fluorescein TSA reagent (1:50 in TSA amplification diluent) for 10 min at RT. TSA blocking reagent, fluorescein TSA reagent, and TSA amplification diluent are part of the TSA detection kit (catalog no. NEL701A001KT, Akoya Biosciences, Marlborough, MA). Sections were washed 3×10 min in TNT buffer, mounted on microscope slides, and coverslipped with Prolong Gold Antifade Reagent with DAPI (Invitrogen, catalog no. P36935). Sections were imaged using a Keyence BZ-X800 fluorescent microscope at $\times 2$ and $\times 20$ magnification.

^{td}Tomato DAB immunostaining

Because ^{td}Tomato signal degrades over time, to create a permanent set of slides for anatomical analysis, we performed immunohistochemistry to label ^{td}Tomato protein permanently. Briefly, fixed, free-floating sections (30 μm) were incubated overnight in monoclonal rabbit anti-RFP, biotin-tagged antibody (1:500; Abcam, catalog no. ab34771). Sections were then washed $3 \times$ with PBS and incubated in streptavidin-conjugated peroxidase (DAB-elite kit) for 1 hr. After incubation with streptavidin, sections were washed $2 \times$ in PBS, then $2 \times$ in 0.1 M NaOAc (pH 6.0), then stained in a solution of 0.1 M NaOAc (pH 6.0) containing nickel ammonium sulfate (3%) and 5 μl of 3% H₂O₂. Sections were

stained for up to 10 min, then washed 2 x in NaOAc (pH 6.0), then in PBS, before being mounted on gelatin coated slides, dehydrated, and coverslipped in DPX. Bright-field images were acquired using a Cytation 5 imager (BioTek Instruments, Winooski, VT). ^{td}Tomato and CRF immunofluorescent labeling: Tissue processing procedures were similar to the immunofluorescent procedures described above. Sections through the amygdala were incubated in antibodies against CRF (rabbit anti-CRF, # rc-68, 1:2000, The Salk Institute) and goat-anti-RFP (1:1000; Rockland, catalog no. 200-101-379). Primary antibodies were detected by secondary anti-rabbit antibody conjugated with Alexa Fluor 488 and anti-goat antibody conjugated with Alexa Fluor 555 (Invitrogen), resulting in ^{td}Tomato protein being visible as red fluorescence and CRF peptide visible as green fluorescence. High-magnification images of the CeA were taken using a Leica (Wetzlar, Germany) Sp5 confocal microscope.

In situ hybridization

All solutions were prepared with DEPC treated water and all tools and surfaces were wiped with RNAzap followed by DEPC treated water. Adult *Crhr1:Cre*^{-td}Tomato rats (3 males and 3 females) were deeply anesthetized with Avertin (2,2,2-tribromoethanol, 1.25% solution, 0.2 ml/10 g BW, IP), then transcardially perfused with PBS followed by 4% PFA in PBS. Brains were removed, fixed in 4% PFA at 4 °C overnight, then equilibrated in 30% sucrose, sectioned into six series of sections (30 μm, coronal sections) on a frozen sliding microtome (SM 2000R, Leica), and stored in PBS at 4 °C. Brain slices were mounted onto glass slides, dried, and went through in situ hybridization (ISH) using a RNAscope Multiplex Fluorescent kit v2 (ACDbio, Newark, CA) following the manufacturer's protocol.

Slice electrophysiology

Following rapid decapitation, brains were extracted and sectioned as previously described (**Herman and Roberto, 2016**). Briefly, brains were placed in ice-cold high sucrose solution containing (in mM): sucrose 206.0; KCl 2.5; CaCl₂ 0.5; MgCl₂ 7.0; NaH₂PO₄ 1.2; NaHCO₃ 26; glucose 5.0; HEPES 5. Coronal sections (300 μm) were prepared on a vibrating microtome (Leica VT1000S, Leica Microsystem) and placed in an incubation chamber with oxygenated (95% O₂/5% CO₂) artificial cerebrospinal fluid (aCSF) containing (in mM): NaCl 120; KCl 2.5; EGTA 5; CaCl₂ 2.0 MgCl₂ 1.0; NaH₂PO₄ 1.2; NaHCO₃ 26; Glucose 1.75; HEPES 5. Slices were incubated for 30 min at 37 °C, followed by a 30 min acclimation at room temperature. Patch pipettes (3–6 MΩ; King Precision Glass Inc, Claremont, CA) were filled with an internal solution containing (in mM): potassium chloride (KCl) 145; EGTA 5; MgCl₂ 5; HEPES 10; Na-ATP 2; Na-GTP 0.2 (for whole cell voltage-clamp recordings) or containing potassium gluconate 145; EGTA 5; MgCl₂ 5; HEPES 10; Na-ATP 2; Na-GTP 0.2 (for whole cell current clamp experimental recordings). Data acquisition was performed with a Multiclamp 700B amplifier (Molecular Devices, San Jose, CA), low-pass filtered at 2–5 kHz, coupled to a digitizer (Digidata 1,550B; Molecular Devices) and stored on a PC using pClamp 10 software (Molecular Devices). Whole-cell voltage-clamp recordings were performed at $V_{\text{hold}} = -60$ mV. Cell-attached recordings were performed with no holding parameters (0 mV). All recordings were performed at room temperature. Series resistance was continuously monitored and cells with series resistance >15 MΩ were excluded from analysis. Properties of sIPSCs were analyzed and visually confirmed using a semi-automated threshold detection program (Minianalysis). The frequency of firing discharge was evaluated and visually confirmed using threshold-based event detection analysis in Clampfit 10.2 (Molecular Devices). Experimental drugs were applied by bath application or y tube for focal application. Analysis was performed on recordings containing >60 events or that encompassed a period of 2–5 min.

Drugs

Clozapine-n-oxide (CNO, NIH Drug Supply Program) was dissolved in 5% DMSO (v/v in saline). CRF was purchased from Tocris Bioscience (Bristol, United Kingdom), dissolved in stock solutions in ultra-pure water, and diluted to final experimental concentration in aCSF.

Crhr1 and *iCre* expression in CeA

The purpose of this experiment was to determine the pattern of ^{td}Tomato protein expression and *Crhr1* and *iCre* mRNA expression within the CeA. Coronal brain sections containing the CeA were processed for immunohistochemical DAB labeling of ^{td}Tomato protein or RNAscope ISH for labeling *Crhr1* and *iCre* mRNA, as described above. A separate set of brain sections containing CeA were processed for

immunofluorescent labeling of ^{td}Tomato and CRF to map the expression pattern of these proteins in the CeA of *Crhr1-Cre-^{td}Tomato* rats. Images were captured using a confocal microscope (model TCS SP5, Leica) and processed with Fiji ImageJ. Coronal sections containing the CeA were identified by neuroanatomical landmarks with reference to a rat brain atlas and captured at ×20 magnification at one single focal plane (1 μm). For analysis of *Crhr1* and *iCre* RNAscope images, punctate signals from each channel were quantified separately following the manufacturer's guideline (ACDbio SOP45-006). Quantification was performed by an experimenter blinded to experimental groups. Based on pilot studies, cells that had more than 3 puncta were considered positive. At least 3 sections representative of the anterior-posterior axis of the CeA were analyzed in each animal.

Membrane properties, inhibitory synaptic transmission, and CRF sensitivity of CeA CRF₁-Cre-^{td}Tomato cells

The purpose of this experiment was to characterize intrinsic properties, inhibitory synaptic transmission, and CRF sensitivity in CRF₁⁺ neurons in the CeA. These neurons were identified using fluorescent optics and brief (< 2 s) episcopic illumination. All labeled neurons were photographed, recorded, and saved. Intrinsic membrane properties were determined in voltage clamp configuration ($V_{\text{hold}} = -60$ mV) using pClamp 10 Clampex software. Current clamp recordings were performed to determine current-voltage (I-V) changes and the firing type of each neuron. Voltage clamp recordings of pharmacologically-isolated GABA_A receptor-mediated spontaneous inhibitory postsynaptic currents (sIPSCs) were performed with bath application of the glutamate receptor blockers 6,7-dinitroquinoline-2,3-dione (DNQX, 20 μM) and DL-2-amino-5-phosphonovalerate (AP-5, 50 μM) and the GABA_B receptor antagonist GCP55845A (1 μM). Cell-attached recordings were made in close juxtacellular (i.e., membrane intact) cell-attached configuration and only cells with regular spontaneous firing were included in analysis. After a stable baseline period, CRF (200 nM) was applied for a period of 7–10 min and changes in firing were measured and compared to baseline. Experiments were performed in individual slices to ensure that drug application was never repeated in the same slice.

Functional validation of Cre-dependent expression of Gq-DREADD receptors in CeA CRF₁-Cre-^{td}Tomato cells

The purpose of this experiment was to test if CeA CRF₁-Cre-^{td}Tomato cells can be activated using chemogenetics via Cre-mediated targeting of Gq-DREADD receptors [hM3D(Gq)] to these cells.

c-Fos validation

To test if Cre-dependent expression of Gq-DREADD receptors can stimulate CeA CRF₁-Cre-^{td}Tomato cells, CRF₁-Cre-^{td}Tomato rats were given bilateral microinjections of AAV8-hSyn-DIO-HA-hM3D(Gq)-IRES-mCitrine (50454-AAV8, Addgene, Watertown, MA) or a control virus (AAV5-hSyn-DIO-EGFP; Addgene, 50457-AAV5) targeting the CeA. Four weeks later, rats were given a systemic CNO injection (4 mg/kg, i.p.) and sacrificed 90 min later. Brain sections (4 sections/rat × 4 rats/group) were processed for c-Fos immunohistochemistry and the percentage of c-Fos⁺ ^{td}Tomato⁺ cells in the CeA was calculated. Cell counts were performed by an experimenter blinded to experimental groups.

Electrophysiological validation

To functionally validate Cre-dependent expression of Gq-DREADD receptors in CeA CRF₁-Cre-^{td}Tomato cells, CRF₁-Cre-^{td}Tomato rats were given bilateral microinjections as described above. After a minimum of 4 weeks, brain slices of CeA were prepared as described above. CeA neuronal expression of mCitrine and ^{td}Tomato were confirmed by fluorescent optics and neurons were targeted for electrophysiological recording. After a stable baseline period, CNO (10 μM) was applied and changes in membrane potential and action potential firing were measured and compared to baseline.

Effects of chemogenetic stimulation of CeA CRF₁-Cre^{-td}Tomato cells on nociception and anxiety-like behavior

The purpose of these experiments was to test the effects of chemogenetic stimulation of CeA CRF₁ cells on nociception and anxiety-like behavior. Rats were given intra-CeA microinjections of AAV8-hSyn-DIO-HA-hM3D(Gq)-IRES-mCitrine (Addgene, 50454-AAV8; Active Virus) or AAV5-hSyn-DIO-EGFP (Addgene, 50457-AAV5; Control Virus) and were given 4 weeks for recovery and viral expression (**Figure 7A**). Please refer to **Figure 7B** for a timeline schematic of this experiment. All rats were habituated to handling before the start of behavioral procedures. On behavioral procedure days, rats were given at least 30 min to acclimate to the procedure room.

Nociception

Mechanical and thermal nociception were measured using the Von Frey (**Pahng et al., 2017**) and Hargreaves (**Avegno et al., 2018**) assays, respectively, as previously described. Briefly, the Von Frey apparatus consists of clear chambers placed on top of a mesh floor. To measure sensitivity to mechanical nociception, each hind paw was perpendicularly stimulated with a Von Frey filament (Electronic Von Frey 38450, Ugo Basile, Gemonio, Italy) calibrated to measure the amount of force applied using the up-down method and the force (g) threshold required to elicit a paw withdrawal response was recorded. Force thresholds were measured twice for each hind paw in alternating fashion, with at least 1 min between measurements, and an average threshold was calculated for each animal. The Hargreaves apparatus consists of clear chambers placed on top of a glass pane suspended above a tabletop. To measure sensitivity to thermal nociception, each hind paw was stimulated by a halogen light heat source (Model 309 Hargreaves Apparatus, IITC Life Sciences, Woodland Hills, CA) and latency (s) for hind paw withdrawal was measured. Withdrawal latencies were measured twice for each hind paw in alternating fashion, with at least 1 min between measurements, and an average withdrawal latency was calculated for each animal.

Baseline paw withdrawal thresholds in the Von Frey assay and withdrawal latencies in the Hargreaves assay were measured over 3 sessions (1 baseline session/day; baseline sessions for each assay occurred on alternating days; **Figure 7B**) that were each preceded 30 min earlier by a vehicle (5% DMSO in saline, i.p.) pretreatment. After the final baseline session, rats were counterbalanced into CNO (4 mg/kg) or Vehicle (5% DMSO) treatment groups based on paw withdrawal latencies during the 3rd (final) Hargreaves baseline session. During Von Frey and Hargreaves test sessions, rats were given CNO (4 mg/kg) or vehicle injections (i.p.) 30 min before the start of testing. All Von Frey and Hargreaves procedures occurred under regular white light illumination.

Anxiety-like behaviors

One day after Hargreaves testing, rats were tested for anxiety-like behaviors in the elevated plus maze (EPM), open field (OF), and light-dark box (LD) on consecutive days (**Figure 7B**). All procedures occurred under indirect, dim illumination (~10 lux). Rats were given CNO (4 mg/kg) or vehicle injections (i.p.) 30 min before the start of each test. The EPM and OF tests were performed as previously described (**Albrechet-Souza et al., 2020; Fucich et al., 2020**). Briefly, the EPM consists of two open and two closed arms elevated 50 cm above the floor. Rats were individually placed in the center of the maze facing an open arm and were given 5 min to explore the maze. Time spent in the open and closed arms of the maze was measured. The OF consists of a square arena with a checkerboard patterned floor (4 × 4 squares). Rats were individually placed in one corner of the arena and were given 5 min to explore the arena. Time spent in the periphery and the center of the arena (defined as the 3 × 3 squares in the center of the arena) was measured. The LD box consists of a two compartments; one with black walls and a black floor, and the other with white walls and a white floor. The black compartment was protected from light (dark box) and the white compartment was illuminated (light box; ~1000 lux). Rats were able to freely explore both dark and light boxes through an opened door. Rats were individually placed in the dark box and were given 5 min to explore the apparatus. Time spent in dark and light boxes, as well as the latency to enter the light box were measured. EPM, OF, and LD tests were recorded via a camera mounted above the apparatus and videos were scored

by an experimenter blinded to treatment groups. At the end of the experiment, rats were sacrificed and brain sections were analyzed for virus placement.

***Crhr1* and *iCre* expression in BLA**

The purpose of this experiment was to examine *Crhr1* and *iCre* mRNA expression in a brain area outside the CeA. The basolateral amygdala (BLA) was selected for analysis because CRF₁ receptors are highly expressed in, and functionally regulate the activity of pyramidal glutamatergic neurons in this area (as opposed to GABAergic neurons in CeA) (Refojo et al., 2011; Rostkowski et al., 2013). Brain sections containing BLA were processed for *Crhr1* and *iCre* RNAscope and analyzed as described above.

Cre^{-td}Tomato fluorescent expression across the brain

The purpose of this experiment was to examine if the Cre^{-td}Tomato transgene is expressed in brain areas outside of the amygdala in a pattern that is consistent with known CRF₁ expression patterns. Male and female (n = 2/sex) CRF₁-Cre^{-td}Tomato rats were perfused transcardially with PBS and 4% PFA, and brains were post-fixed in 4% PFA overnight. Brains were cryoprotected, snap-frozen, and sectioned with a cryostat. Coronal sections (40 μm) were collected across the rostrocaudal axis, mounted onto microscope slides, and coverslipped with Fluorogel-II containing DAPI (Electron Microscopy Sciences). Brain sections were imaged using a Keyence BZ-X800 fluorescent microscope. For each brain region, at least three sections were analyzed.

Statistical analyses

Electrophysiology data on frequency and amplitude of spontaneous inhibitory postsynaptic currents (sIPSCs) were analyzed and manually confirmed using a semi-automated threshold-based detection software (Mini Analysis, Synaptosoft Inc, Decatur, GA). Cell-attached firing discharge data were analyzed and manually confirmed using a semi-automated threshold-based detection software (Clampfit 10.6, Molecular Devices). Electrophysiological characteristics were determined from baseline and experimental drug application containing a minimum of 65 events each. Event data were represented as mean ± SEM or mean % change from baseline ± SEM and analyzed for independent significance using a one-sample t-test, compared by paired or unpaired t-test where appropriate. Data analysis and visualization were completed using Prism 7.0 (GraphPad, San Diego, CA). Behavioral data were analyzed using multifactorial repeated measures ANOVAs (for Von Frey and Hargreaves tests) or t-tests (for anxiety tests). For RM ANOVAs, between-subjects factors include sex and treatment, and the within-subjects repeated measure was test session (i.e. baseline vs. test). Data from the active and control virus groups were analyzed separately (i.e. the control virus group was treated as a replication of the experiment; Weera et al., 2021). Data from experiments that only have two groups (e.g. c-Fos immunohistochemistry) were analyzed using t-tests. Data were analyzed using the Statistical Package for Social Sciences (Version 25, IBM Corporation, Armonk, NY). Statistical significance was set at p < 0.05.

Acknowledgements

This work was supported by National Institutes of Health Grants AA023305 (NWG), AA026022 (to NWG and MAH), AA023002 (MAH), AA027145 (MMW), and AA007577 (institutional NRSA training grant that supported MMW). This work was also supported in part by a Merit Review Award #101 BX003451 (to NWG) from the United States Department of Veterans Affairs, Biomedical Laboratory Research and Development Service.

Additional information

Funding

Funder	Grant reference number	Author
National Institute on Alcohol Abuse and Alcoholism	R01 AA023305	Nicholas W Gilpin
National Institute on Alcohol Abuse and Alcoholism	R21 AA026022	Melissa Herman Nicholas W Gilpin
National Institute on Alcohol Abuse and Alcoholism	R00 AA023002	Melissa Herman
National Institute on Alcohol Abuse and Alcoholism	National Research Service Award AA027145	Marcus M Weera
National Institute on Alcohol Abuse and Alcoholism	Institutional Training Grant AA007577	Marcus M Weera
United States Department of Veterans Affairs	Merit Award #I01 BX003451	Nicholas W Gilpin

The funders had no role in study design, data collection and interpretation, or the decision to submit the work for publication.

Author contributions

Marcus M Weera, Conceptualization, Data curation, Formal analysis, Funding acquisition, Investigation, Methodology, Project administration, Writing – original draft, Writing – review and editing; Abigail E Agoglia, Data curation, Formal analysis, Investigation, Writing – original draft; Eliza Douglass, Rosetta S Shackett, Data curation, Investigation; Zhiying Jiang, Shivakumar Rajamanickam, Data curation, Formal analysis, Investigation; Melissa A Herman, Conceptualization, Data curation, Formal analysis, Funding acquisition, Investigation, Methodology, Project administration, Resources, Supervision, Validation, Visualization, Writing – original draft, Writing – review and editing; Nicholas J Justice, Conceptualization, Funding acquisition, Investigation, Project administration, Resources, Supervision, Validation, Writing – review and editing; Nicholas W Gilpin, Conceptualization, Funding acquisition, Project administration, Resources, Supervision, Writing – review and editing

Author ORCIDs

Marcus M Weera  <http://orcid.org/0000-0002-2451-0350>
 Nicholas W Gilpin  <http://orcid.org/0000-0001-8901-8917>

Ethics

All animal procedures were conducted in accordance with recommendations in the Guide for the Care and Use of Laboratory Animals of the National Institutes of Health, and were approved by the Institutional Animal Care and Use Committee of the respective institutions at which procedures occurred (Louisiana State University Health Sciences Center, University of North Carolina - Chapel Hill, University of Texas Health Sciences Center). (LSUHSC IACUC Protocol #3749; UNC IACUC Protocol #19-190; UTHSC IACUC Protocol #21-075).

Decision letter and Author response

Decision letter <https://doi.org/10.7554/eLife.67822.sa1>

Author response <https://doi.org/10.7554/eLife.67822.sa2>

Additional files

Supplementary files

- Transparent reporting form

- Source data 1. Slice electrophysiology data.
- Source data 2. Behavioral data.

Data availability

All data generated during this study are included in the manuscript.

References

- Agoglia AE**, Tella J, Herman MA. 2020. Sex differences in corticotropin releasing factor peptide regulation of inhibitory control and excitability in central amygdala corticotropin releasing factor receptor 1-neurons. *Neuropharmacology* **180**:108296. DOI: <https://doi.org/10.1016/j.neuropharm.2020.108296>, PMID: 32950560
- Albrechet-Souza L**, Schratz CL, Gilpin NW. 2020. Sex differences in traumatic stress reactivity in rats with and without a history of alcohol drinking. *Biology of Sex Differences* **11**:27. DOI: <https://doi.org/10.1186/s13293-020-00303-w>, PMID: 32393336
- Andreoli M**, Marketkar T, Dimitrov E. 2017. Contribution of amygdala CRF neurons to chronic pain. *Experimental Neurology* **298**:1–12. DOI: <https://doi.org/10.1016/j.expneurol.2017.08.010>, PMID: 28830762
- Avegno EM**, Lobell TD, Itoga CA, Baynes BB, Whitaker AM, Weera MM, Edwards S, Middleton JW, Gilpin NW. 2018. Central Amygdala Circuits Mediate Hyperalgesia in Alcohol-Dependent Rats. *The Journal of Neuroscience* **38**:7761–7773. DOI: <https://doi.org/10.1523/JNEUROSCI.0483-18.2018>, PMID: 30054393
- Chieng BCH**, Christie MJ, Osborne PB. 2006. Characterization of neurons in the rat central nucleus of the amygdala: cellular physiology, morphology, and opioid sensitivity. *The Journal of Comparative Neurology* **497**:910–927. DOI: <https://doi.org/10.1002/cne.21025>, PMID: 16802333
- Cohen A**, Treweek J, Edwards S, Leão RM, Schulteis G, Koob GF, George O. 2015. Extended access to nicotine leads to a CRF1 receptor dependent increase in anxiety-like behavior and hyperalgesia in rats. *Addiction* **20**:56–68. DOI: <https://doi.org/10.1111/adb.12077>, PMID: 23869743
- Commons KG**, Connolley KR, Valentino RJ. 2003. A neurochemically distinct dorsal raphe-limbic circuit with a potential role in affective disorders. *Neuropsychopharmacology* **28**:206–215. DOI: <https://doi.org/10.1038/sj.npp.1300045>, PMID: 12589373
- Crawley JN**, Davis LG. 1982. Baseline exploratory activity predicts anxiolytic responsiveness to diazepam in five mouse strains. *Brain Research Bulletin* **8**:609–612. DOI: [https://doi.org/10.1016/0361-9230\(82\)90087-9](https://doi.org/10.1016/0361-9230(82)90087-9), PMID: 6890398
- Dabrowska J**, Martinon D, Moaddab M, Rainnie DG. 2016. Targeting Corticotropin-Releasing Factor Projections from the Oval Nucleus of the Bed Nucleus of the Stria Terminalis Using Cell-Type Specific Neuronal Tracing Studies in Mouse and Rat Brain. *Journal of Neuroendocrinology* **28**:12442. DOI: <https://doi.org/10.1111/jne.12442>, PMID: 27805752
- Day HE**, Curran EJ, Watson SJ, Akil H. 1999. Distinct neurochemical populations in the rat central nucleus of the amygdala and bed nucleus of the stria terminalis: evidence for their selective activation by interleukin-1beta. *The Journal of Comparative Neurology* **413**:113–128. PMID: 10464374.
- Dedic N**, Chen A, Deussing JM. 2018. The CRF Family of Neuropeptides and their Receptors - Mediators of the Central Stress Response. *Current Molecular Pharmacology* **11**:4–31. DOI: <https://doi.org/10.2174/1874467210666170302104053>, PMID: 28260504
- Duvarci S**, Pare D. 2014. Amygdala microcircuits controlling learned fear. *Neuron* **82**:966–980. DOI: <https://doi.org/10.1016/j.neuron.2014.04.042>, PMID: 24908482
- Edwards S**, Vendruscolo LF, Schlosburg JE, Misra KK, Wee S, Park PE, Schulteis G, Koob GF. 2012. Development of mechanical hypersensitivity in rats during heroin and ethanol dependence: alleviation by CRF₁ receptor antagonism. *Neuropharmacology* **62**:1142–1151. DOI: <https://doi.org/10.1016/j.neuropharm.2011.11.006>, PMID: 22119954
- Fadok JP**, Krabbe S, Markovic M, Courtin J, Xu C, Massi L, Botta P, Bylund K, Müller C, Kovacevic A, Tovote P, Lüthi A. 2017. A competitive inhibitory circuit for selection of active and passive fear responses. *Nature* **542**:96–100. DOI: <https://doi.org/10.1038/nature21047>, PMID: 28117439
- File SE**, Lippa AS, Beer B, Lippa MT. 2004. Animal tests of anxiety. *Current Protocols in Neuroscience* **8**:26. DOI: <https://doi.org/10.1002/0471142301.ns0803s26>, PMID: 18428606
- Fucich EA**, Stielper ZF, Cancienne HL, Edwards S, Gilpin NW, Molina PE, Middleton JW. 2020. Endocannabinoid degradation inhibitors ameliorate neuronal and synaptic alterations following traumatic brain injury. *Journal of Neurophysiology* **123**:707–717. DOI: <https://doi.org/10.1152/jn.00570.2019>, PMID: 31913777
- Gilpin NW**, Herman MA, Roberto M. 2015. The central amygdala as an integrative hub for anxiety and alcohol use disorders. *Biological Psychiatry* **77**:859–869. DOI: <https://doi.org/10.1016/j.biopsych.2014.09.008>
- Glover CPJ**, Bienemann AS, Heywood DJ, Cosgrave AS, Uney JB. 2002. Adenoviral-mediated, high-level, cell-specific transgene expression: A SYN1-WPRE cassette mediates increased transgene expression with no loss of neuron specificity. *Molecular Therapy: The Journal of the American Society of Gene Therapy* **5**:509–516. DOI: <https://doi.org/10.1006/mthe.2002.0588>
- Henckens MJAG**, Deussing JM, Chen A. 2016. Region-specific roles of the corticotropin-releasing factor-urocortin system in stress. *Nature Reviews. Neuroscience* **17**:636–651. DOI: <https://doi.org/10.1038/nrn.2016.94>, PMID: 27586075

- Henry B**, Vale W, Markou A. 2006. The effect of lateral septum corticotropin-releasing factor receptor 2 activation on anxiety is modulated by stress. *The Journal of Neuroscience* **26**:9142–9152. DOI: <https://doi.org/10.1523/JNEUROSCI.1494-06.2006>, PMID: 16957071
- Herman MA**, Contet C, Justice NJ, Vale W, Roberto M. 2013. Novel subunit-specific tonic GABA currents and differential effects of ethanol in the central amygdala of CRF receptor-1 reporter mice. *The Journal of Neuroscience* **33**:3284–3298. DOI: <https://doi.org/10.1523/JNEUROSCI.2490-12.2013>, PMID: 23426657
- Herman MA**, Contet C, Roberto M. 2016. A Functional Switch in Tonic GABA Currents Alters the Output of Central Amygdala Corticotropin Releasing Factor Receptor-1 Neurons Following Chronic Ethanol Exposure. *The Journal of Neuroscience* **36**:10729–10741. DOI: <https://doi.org/10.1523/JNEUROSCI.1267-16.2016>, PMID: 27798128
- Herman MA**, Roberto M. 2016. Cell-type-specific tonic GABA signaling in the rat central amygdala is selectively altered by acute and chronic ethanol. *Addiction Biology* **21**:72–86. DOI: <https://doi.org/10.1111/adb.12181>, PMID: 25170988
- Homberg JR**, Wöhr M, Alenina N. 2017. Comeback of the Rat in Biomedical Research. *ACS Chemical Neuroscience* **8**:900–903. DOI: <https://doi.org/10.1021/acschemneuro.6b00415>, PMID: 28182397
- Hunt AJ**, Dasgupta R, Rajamanickam S, Jiang Z, Beierlein M, Chan CS, Justice NJ. 2018. Paraventricular hypothalamic and amygdalar CRF neurons synapse in the external globus pallidus. *Brain Structure & Function* **223**:2685–2698. DOI: <https://doi.org/10.1007/s00429-018-1652-y>, PMID: 29569009
- Itoga CA**, Roltsch Hellard EA, Whitaker AM, Lu YL, Schreiber AL, Baynes BB, Baiamonte BA, Richardson HN, Gilpin NW. 2016. Traumatic Stress Promotes Hyperalgesia via Corticotropin-Releasing Factor-1 Receptor (CRFR1) Signaling in Central Amygdala. *Neuropsychopharmacology* **41**:2463–2472. DOI: <https://doi.org/10.1038/npp.2016.44>, PMID: 27013358
- Iwasaki-Sekino A**, Mano-Otagiri A, Ohata H, Yamauchi N, Shibasaki T. 2009. Gender differences in corticotropin and corticosterone secretion and corticotropin-releasing factor mRNA expression in the paraventricular nucleus of the hypothalamus and the central nucleus of the amygdala in response to footshock stress or psychological stress in rats. *Psychoneuroendocrinology* **34**:226–237. DOI: <https://doi.org/10.1016/j.psyneuen.2008.09.003>, PMID: 18849120
- Ji G**, Neugebauer V. 2007. Differential effects of CRF1 and CRF2 receptor antagonists on pain-related sensitization of neurons in the central nucleus of the amygdala. *Journal of Neurophysiology* **97**:3893–3904. DOI: <https://doi.org/10.1152/jn.00135.2007>, PMID: 17392412
- Ji G**, Neugebauer V. 2008. Pro- and anti-nociceptive effects of corticotropin-releasing factor (CRF) in central amygdala neurons are mediated through different receptors. *Journal of Neurophysiology* **99**:1201–1212. DOI: <https://doi.org/10.1152/jn.01148.2007>, PMID: 18171711
- Ji G**, Fu Y, Adwanikar H, Neugebauer V. 2013. Non-pain-related CRF1 activation in the amygdala facilitates synaptic transmission and pain responses. *Molecular Pain* **9**:2. DOI: <https://doi.org/10.1186/1744-8069-9-2>, PMID: 23410057
- Jiang Z**, Rajamanickam S, Justice NJ. 2018. Local Corticotropin-Releasing Factor Signaling in the Hypothalamic Paraventricular Nucleus. *The Journal of Neuroscience* **38**:1874–1890. DOI: <https://doi.org/10.1523/JNEUROSCI.1492-17.2017>, PMID: 29352046
- Jolkkonen E**, Pitkänen A. 1998. Intrinsic connections of the rat amygdaloid complex: projections originating in the central nucleus. *The Journal of Comparative Neurology* **395**:53–72. DOI: [https://doi.org/10.1002/\(sici\)1096-9861\(19980525\)395:1<53::aid-cne5>3.0.co;2-g](https://doi.org/10.1002/(sici)1096-9861(19980525)395:1<53::aid-cne5>3.0.co;2-g), PMID: 9590546
- Justice NJ**, Yuan ZF, Sawchenko PE, Vale W. 2008. Type 1 corticotropin-releasing factor receptor expression reported in BAC transgenic mice: implications for reconciling ligand-receptor mismatch in the central corticotropin-releasing factor system. *The Journal of Comparative Neurology* **511**:479–496. DOI: <https://doi.org/10.1002/cne.21848>, PMID: 18853426
- Koresawa Y**, Miyagawa S, Ikawa M, Matsunami K, Yamada M, Shirakura R, Okabe M. 2000. Synthesis of a new Cre recombinase gene based on optimal codon usage for mammalian systems. *Journal of Biochemistry* **127**:367–372. DOI: <https://doi.org/10.1093/oxfordjournals.jbchem.a022617>, PMID: 10731707
- Liu P**, Jenkins NA, Copeland NG. 2003. A highly efficient recombineering-based method for generating conditional knockout mutations. *Genome Research* **13**:476–484. DOI: <https://doi.org/10.1101/gr.749203>, PMID: 12618378
- Merlo Pich E**, Lorang M, Yeganeh M, Rodriguez de Fonseca F, Raber J, Koob GF, Weiss F. 1995. Increase of extracellular corticotropin-releasing factor-like immunoreactivity levels in the amygdala of awake rats during restraint stress and ethanol withdrawal as measured by microdialysis. *The Journal of Neuroscience* **15**:5439–5447. DOI: <https://doi.org/10.1523/JNEUROSCI.15-08-05439.1995>, PMID: 7643193
- Milan-Lobo L**, Gsandtner I, Gaubitzer E, Rünzler D, Buchmayer F, Köhler G, Bonci A, Freissmuth M, Sitte HH. 2009. Subtype-specific differences in corticotropin-releasing factor receptor complexes detected by fluorescence spectroscopy. *Molecular Pharmacology* **76**:1196–1210. DOI: <https://doi.org/10.1124/mol.109.059139>, PMID: 19755522
- Mohammad F**, Ho J, Woo JH, Lim CL, Poon DJJ, Lamba B, Claridge-Chang A. 2016. Concordance and incongruence in preclinical anxiety models: Systematic review and meta-analyses. *Neuroscience and Biobehavioral Reviews* **68**:504–529. DOI: <https://doi.org/10.1016/j.neubiorev.2016.04.011>, PMID: 27328783
- Pahng AR**, Paulsen RI, McGinn MA, Edwards KN, Edwards S. 2017. Neurobiological Correlates of Pain Avoidance-Like Behavior in Morphine-Dependent and Non-Dependent Rats. *Neuroscience* **366**:1–14. DOI: <https://doi.org/10.1016/j.neuroscience.2017.09.055>, PMID: 29024786

- Peng J**, Long B, Yuan J, Peng X, Ni H, Li X, Gong H, Luo Q, Li A. 2017. A Quantitative Analysis of the Distribution of CRH Neurons in Whole Mouse Brain. *Frontiers in Neuroanatomy* **11**:63. DOI: <https://doi.org/10.3389/fnana.2017.00063>, PMID: 28790896
- Pomrenze MB**, Millan EZ, Hopf FW, Keiflin R, Maiya R, Blasio A, Dadgar J, Kharazia V, De Guglielmo G, Crawford E, Janak PH, George O, Rice KC, Messing RO. 2015. A Transgenic Rat for Investigating the Anatomy and Function of Corticotrophin Releasing Factor Circuits. *Frontiers in Neuroscience* **9**:487. DOI: <https://doi.org/10.3389/fnins.2015.00487>, PMID: 26733798
- Pomrenze MB**, Giovanetti SM, Maiya R, Gordon AG, Kreeger LJ, Messing RO. 2019. Dissecting the Roles of GABA and Neuropeptides from Rat Central Amygdala CRF Neurons in Anxiety and Fear Learning. *Cell Reports* **29**:13–21. DOI: <https://doi.org/10.1016/j.celrep.2019.08.083>, PMID: 31577943
- Potter E**, Sutton S, Donaldson C, Chen R, Perrin M, Lewis K, Sawchenko PE, Vale W. 1994. Distribution of corticotropin-releasing factor receptor mRNA expression in the rat brain and pituitary. *PNAS* **91**:8777–8781. DOI: <https://doi.org/10.1073/pnas.91.19.8777>, PMID: 8090722
- Rassnick S**, Heinrichs SC, Britton KT, Koob GF. 1993. Microinjection of a corticotropin-releasing factor antagonist into the central nucleus of the amygdala reverses anxiogenic-like effects of ethanol withdrawal. *Brain Research* **605**:25–32. DOI: [https://doi.org/10.1016/0006-8993\(93\)91352-s](https://doi.org/10.1016/0006-8993(93)91352-s), PMID: 8467387
- Refojo D**, Schweizer M, Kuehne C, Ehrenberg S, Thoeringer C, Vogl AM, Dedic N, Schumacher M, von Wolff G, Avrabos C, Touma C, Engblom D, Schütz G, Nave K-A, Eder M, Wotjak CT, Sillaber I, Holsboer F, Wurst W, Deussing JM. 2011. Glutamatergic and dopaminergic neurons mediate anxiogenic and anxiolytic effects of CRHR1. *Science (New York, N.Y.)* **333**:1903–1907. DOI: <https://doi.org/10.1126/science.1202107>, PMID: 21885734
- Roberto M**, Cruz MT, Gilpin NW, Sabino V, Schweitzer P, Bajo M, Cottone P, Madamba SG, Stouffer DG, Zorrilla EP, Koob GF, Siggins GR, Parsons LH. 2010. Corticotropin releasing factor-induced amygdala gamma-aminobutyric Acid release plays a key role in alcohol dependence. *Biological Psychiatry* **67**:831–839. DOI: <https://doi.org/10.1016/j.biopsych.2009.11.007>, PMID: 20060104
- Rostkowski AB**, Leitermann RJ, Urban JH. 2013. Differential activation of neuronal cell types in the basolateral amygdala by corticotropin releasing factor. *Neuropeptides* **47**:273–280. DOI: <https://doi.org/10.1016/j.npep.2012.12.004>, PMID: 23688647
- Sanford CA**, Soden ME, Baird MA, Miller SM, Schulkin J, Palmiter RD, Clark M, Zweifel LS. 2017. A Central Amygdala CRF Circuit Facilitates Learning about Weak Threats. *Neuron* **93**:164–178. DOI: <https://doi.org/10.1016/j.neuron.2016.11.034>, PMID: 28017470
- Scholl JL**, Afzal A, Fox LC, Watt MJ, Forster GL. 2019. Sex differences in anxiety-like behaviors in rats. *Physiology & Behavior* **211**:112670. DOI: <https://doi.org/10.1016/j.physbeh.2019.112670>, PMID: 31487491
- Shaner NC**, Campbell RE, Steinbach PA, Giepmans BNG, Palmer AE, Tsien RY. 2004. Improved monomeric red, orange and yellow fluorescent proteins derived from *Discosoma* sp. red fluorescent protein. *Nature Biotechnology* **22**:1567–1572. DOI: <https://doi.org/10.1038/nbt1037>, PMID: 15558047
- Smith SM**, Vale WW. 2006. The role of the hypothalamic-pituitary-adrenal axis in neuroendocrine responses to stress. *Dialogues in Clinical Neuroscience* **8**:383–395. DOI: <https://doi.org/10.31887/DCNS.2006.8.4/ssmith>, PMID: 17290797
- STAR Consortium**, Saar K, Beck A, Bihoreau M-T, Birney E, Brocklebank D, Chen Y, Cuppen E, Demonchy S, Dopazo J, Flicek P, Foglio M, Fujiyama A, Gut IG, Gauguier D, Guigo R, Guryev V, Heinig M, Hummel O, Jahn N, et al. 2008. SNP and haplotype mapping for genetic analysis in the rat. *Nature Genetics* **40**:560–566. DOI: <https://doi.org/10.1038/ng.124>, PMID: 18443594
- Vale W**, Spiess J, Rivier C, Rivier J. 1981. Characterization of a 41-residue ovine hypothalamic peptide that stimulates secretion of corticotropin and beta-endorphin. *Science (New York, N.Y.)* **213**:1394–1397. DOI: <https://doi.org/10.1126/science.6267699>, PMID: 6267699
- Van Pett K**, Viau V, Bittencourt JC, Chan RK, Li HY, Arias C, Prins GS, Perrin M, Vale W, Sawchenko PE. 2000. Distribution of mRNAs encoding CRF receptors in brain and pituitary of rat and mouse. *The Journal of Comparative Neurology* **428**:191–212. DOI: [https://doi.org/10.1002/1096-9861\(20001211\)428:2<191::aid-cne1>3.0.co;2-u](https://doi.org/10.1002/1096-9861(20001211)428:2<191::aid-cne1>3.0.co;2-u), PMID: 11064361
- Wanat MJ**, Hopf FW, Stuber GD, Phillips PEM, Bonci A. 2008. Corticotropin-releasing factor increases mouse ventral tegmental area dopamine neuron firing through a protein kinase C-dependent enhancement of Ih. *The Journal of Physiology* **586**:2157–2170. DOI: <https://doi.org/10.1113/jphysiol.2007.150078>, PMID: 18308824
- Weathington JM**, Hamki A, Cooke BM. 2014. Sex- and region-specific pubertal maturation of the corticotropin-releasing factor receptor system in the rat. *The Journal of Comparative Neurology* **522**:1284–1298. DOI: <https://doi.org/10.1002/cne.23475>, PMID: 24115088
- Weera MM**, Schreiber AL, Avegno EM, Gilpin NW. 2020. The role of central amygdala corticotropin-releasing factor in predator odor stress-induced avoidance behavior and escalated alcohol drinking in rats. *Neuropharmacology* **166**:107979. DOI: <https://doi.org/10.1016/j.neuropharm.2020.107979>, PMID: 32028150
- Weera MM**, Shackett RS, Kramer HM, Middleton JW, Gilpin NW. 2021. Central Amygdala Projections to Lateral Hypothalamus Mediate Avoidance Behavior in Rats. *The Journal of Neuroscience* **41**:61–72. DOI: <https://doi.org/10.1523/JNEUROSCI.0236-20.2020>, PMID: 33188067
- Zorrilla EP**, Valdez GR, Weiss F. 2001. Changes in levels of regional CRF-like-immunoreactivity and plasma corticosterone during protracted drug withdrawal in dependent rats. *Psychopharmacology* **158**:374–381. DOI: <https://doi.org/10.1007/s002130100773>, PMID: 11797058